

# Quantum-gravity effects on a Higgs-Yukawa model

Astrid Eichhorn,<sup>1</sup> Aaron Held,<sup>2</sup> and Jan M. Pawłowski<sup>2,3</sup>

<sup>1</sup>*Blackett Laboratory, Imperial College, London SW7 2AZ, United Kingdom*

<sup>2</sup>*Institut für Theoretische Physik, Universität Heidelberg, Philosophenweg 16, 69120 Heidelberg, Germany*

<sup>3</sup>*ExtreMe Matter Institute EMMI, GSI, Planckstr. 1, D-64291 Darmstadt, Germany*

A phenomenologically viable theory of quantum gravity must accommodate all observed matter degrees of freedom and their properties. Here, we explore whether a toy model of the Higgs-Yukawa sector of the Standard Model is compatible with asymptotically safe quantum gravity. We discuss the phenomenological implications of our result in the context of the Standard Model.

We analyze the quantum scaling dimension of the system, and find an irrelevant Yukawa coupling at a joint gravity-matter fixed point. Further, we explore the impact of gravity-induced couplings between scalars and fermions, which are non-vanishing in asymptotically safe gravity.

## I. INTRODUCTION

Asymptotic safety [1] provides a framework in which a local quantum field theory of the metric - or related gravitational degrees of freedom, such as, e.g., the vielbein - could be established. Compelling hints for the viability of the asymptotic-safety scenario have been uncovered in pure gravity [2–44], for reviews see [45–51]; similar ideas have been explored in other quantum field theories, see, e.g., [52–54]. These results suggest that quantum fluctuations of gravity could induce an interacting Renormalization Group (RG) fixed point, generalizing the success-story of asymptotic freedom to a quantum gravitational setting. Yet, a fundamental model of spacetime that is viable in our universe must be compatible with the existence and properties of the observed matter degrees of freedom. First results suggest that asymptotic safety in gravity persists if the matter fields of the Standard Model and some of its extensions are coupled minimally to gravity [55–58]. Here, we focus on the converse question, namely the effect of quantum gravity on matter fields and their interactions in the ultraviolet (UV). The Standard Model is a low-energy effective field theory, which presumably features perturbative Landau poles and a trivality problem beyond perturbation theory in the Higgs sector and the U(1) hypercharge sector. Within the asymptotic-safety scenario local quantum field theory remains a valid framework up to arbitrarily high momentum scales, requiring a quantum-gravity induced Renormalization Group fixed point for matter. First hints for its existence have been found in [59–69].

In this work, we focus on a toy model of the Yukawa sector of the Standard Model, a matter system with a massless Dirac fermion and a real scalar interacting via a Yukawa term with coupling  $y$ , in the presence of quantum gravity. Within canonical power counting, the Yukawa coupling  $y$  corresponds to a marginally irrelevant coupling. If the coupled matter-gravity system is asymptotically safe and the Yukawa coupling remains irrelevant, this results in a prediction for the low-energy limit: The value of the latter is dominated by the UV-relevant couplings in the vicinity of the UV-fixed point, which deter-

mine the RG-trajectory from the UV-regime to the low energy regime. In turn, UV-irrelevant couplings correspond to a UV-repulsive direction of a fixed point, and their value governs the approach to the critical surface at low energies. Thus, in this scenario most values of  $y$  in the infrared (IR) are incompatible with asymptotic safety.

In this spirit it has been conjectured that the Higgs mass could be predicted within asymptotic safety [70, 71]. Two conditions need to be satisfied for this scenario to work in the Standard Model: Firstly, the Higgs self-interaction must become irrelevant at the fixed point. Secondly, the top-Yukawa coupling needs to be relevant, if the corresponding fixed point lies at a vanishing value of the coupling. Otherwise, the UV-repulsive fixed point at  $y = 0$  is difficult to reconcile with the value of the top-Yukawa coupling at the Planck scale, which is significantly larger than zero in the Standard Model [72].

The main goals of this paper are the following two: Firstly, we study the quantum gravitational correction to the critical exponent of the Yukawa coupling at its fixed point to determine whether the low-energy value of the Yukawa coupling could be predicted in a matter-gravity model in Section III. Secondly, we take a more detailed look at the properties of a joint matter-gravity fixed point. In particular, we focus on quantum-gravity induced interactions, and the shift of a possible matter fixed point to an asymptotically safe instead of an asymptotically free one in Section IV.

## II. YUKAWA THEORY COUPLED TO QUANTUM GRAVITY

### A. Effective action

We will analyze the momentum-scale running of the effective action  $\Gamma_k$  of a Yukawa theory coupled to gravity in the presence of an infrared cutoff scale  $k$ . More specifically, we will monitor the scale-dependence of matter couplings in the vicinity of the asymptotically safe UV fixed point of the theory. The theory consists of a Dirac fermion  $\psi$  and a real scalar  $\phi$  coupled to a fluctuating

metric. The flowing action  $\Gamma_k$  of the model is parameterized as

$$\begin{aligned} \Gamma_k[\bar{g}, \Phi] = & \frac{Z_\phi}{2} \int d^4x \sqrt{\bar{g}} (g^{\mu\nu} \partial_\mu \phi \partial_\nu \phi + m_\phi^2 \phi^2) \\ & + iZ_\psi \int d^4x \sqrt{\bar{g}} \bar{\psi} \not{\nabla} \psi \\ & + iZ_\psi Z_\phi^{1/2} y \int d^4x \sqrt{\bar{g}} \phi \bar{\psi} \psi \\ & + \Gamma_{k,\text{ho}}[\bar{g}, \Phi] + \Gamma_{k,\text{grav}}[\bar{g}, \Phi], \end{aligned} \quad (1)$$

with scale-dependent couplings  $y(k)$  and  $m_\phi^2(k)$  and wave-function renormalizations  $Z_\phi(k)$ ,  $Z_\psi(k)$ . The Dirac term contains the spin connection, see App. E. The effective action depends on an auxiliary background metric  $\bar{g}_{\mu\nu}$  and the fluctuating quantum fields  $\Phi$  with

$$\Phi = (h_{\mu\nu}, c_\nu, \bar{c}_\nu, \psi, \bar{\psi}, \phi). \quad (2)$$

In (2) the field  $h$  carries the metric fluctuations and the corresponding pure-gravity dynamics is contained in  $\Gamma_{k,\text{grav}}$ . The full metric  $g_{\mu\nu} = g_{\mu\nu}(\bar{g}, h)$  in the first three lines of (1) is chosen to be

$$g_{\mu\nu} = Z_{\bar{g}}^{1/2} \bar{g}_{\mu\nu} + \sqrt{G} Z_h^{1/2} h_{\mu\nu}, \quad (3)$$

with Newton coupling  $G$ . The wave function renormalizations  $Z_{\bar{g}}$  and  $Z_h$  carry the cutoff-scale dependence of the respective kinetic terms similar to those of the scalar and fermion. The parameterization (1) with (3) leaves us with RG-invariant but scale-dependent couplings  $y$  and  $G$ , while the RG-scaling of the vertices is carried entirely by the corresponding  $Z$ -factors. The factor  $\sqrt{G}$  leaves the fluctuation field  $h$  with the canonical dimension of a bosonic field such that powers of  $G$  occur in all matter-gravity and pure-gravity vertices.

The presence of the background metric is required for two reasons: Firstly, the use of an RG-approach in gravity requires to set a scale in order to distinguish the ‘‘high-momentum modes’’ of the model. This is possible with the help of the background-covariant Laplacian. Secondly, our approach requires the specification of a propagator for the metric, which, as in any gauge theory, requires the introduction of a gauge-fixing term. Here, we will use a family of gauge fixing functionals with respect to the background metric.

In the present setting classical diffeomorphism invariance is encoded in Slavnov-Taylor identities. They imply that the quantum effective action cannot be expanded in diffeomorphism-invariant terms. This entails that the first three lines in (1) are accompanied by higher order terms  $\Gamma_{k,\text{ho}}$  dictated by the Slavnov-Taylor identities. These terms are neglected in the present work. A more detailed discussion of background independence is given in App. A.

The propagator of metric fluctuations is obtained from the Einstein-Hilbert action with general covariant gauges

and the same linear metric split, cf. (3). The classical action reads

$$S_{\text{EH}} = \frac{1}{16\pi G} \int d^4x \sqrt{\bar{g}} (2\Lambda - R) + S_{\text{gf}} + S_{\text{gh}}. \quad (4)$$

and we employ the linear gauge fixing condition

$$F_\mu = \left( \delta_\mu^\rho \bar{D}^\sigma - \frac{1-\beta}{4} \bar{g}^{\rho\sigma} \bar{D}_\mu \right) h_{\rho\sigma}, \quad (5)$$

where  $\bar{D}$  is the covariant derivative w.r.t. the background metric  $\bar{g}_{\mu\nu}$ . This results in a gauge-fixing term,

$$S_{\text{gf}} = \frac{1}{32\pi G\alpha} \int d^4x \sqrt{\bar{g}} \bar{g}^{\mu\nu} F_\mu F_\nu, \quad (6)$$

accompanied by the standard Faddeev-Popov-ghost term. We thus have a two-parameter family of gauges labelled by  $(\alpha, \beta)$ . Given an expansion in powers of the fluctuating graviton  $h$ , we obtain the quadratic part of the pure-gravity effective action from which we construct the scale-dependent full metric propagator, for details see App. C. In the present work we will not evaluate the gravitational RG flow explicitly, but instead utilize results for pure quantum gravity, and quantum gravity coupled to free matter. Thus gravitational couplings such as  $G$  and the graviton-mass parameter  $\mu_h$  constitute free parameters of our equations.

We close this Section with a discussion of the global symmetries of the model in (1). The kinetic terms of the scalar and fermion feature a separate  $\mathbb{Z}_2$  symmetry under which  $\phi \rightarrow -\phi$ , and a chiral symmetry in the fermion sector under which  $\psi \rightarrow e^{i\gamma_5 \vartheta} \psi$  and  $\bar{\psi} \rightarrow \bar{\psi} e^{i\gamma_5 \vartheta}$ . The Yukawa coupling reduces these separate symmetries to a combined discrete chiral symmetry under which the scalar and the fermions transform simultaneously and  $\vartheta = \pi/2$ . It has the same effect a global chiral symmetry would have in the Standard Model, forbidding a fermionic mass term. Further, it restricts the type of self-interactions that can be induced by quantum gravity. All induced interactions respect the global symmetries of the matter sector; in particular the *separate* symmetries of the fermionic and scalar kinetic terms, as these provide the vertices that source the induced interactions. Note that it would be interesting to understand whether the general argument, that black-hole configurations in the quantum gravitational path integral lead to the breaking of global symmetries [73] also applies in asymptotic safety and if the preservation of global symmetries that we observe is an artifact of the truncation or our choice of background and/or signature.

## B. Functional renormalization group approach

To explore the scale-dependence of our matter-gravity theory we employ the non-perturbative functional Renormalization Group (FRG) approach, for reviews see [74–82].

In this approach the theory is regularized in the infrared below a momentum scale  $k$ . This is achieved with an infrared regulator term in the classical action that underlies the generating functional,

$$S_{\text{cl}} \rightarrow S_{\text{cl}} + \frac{1}{2} \int_x \sqrt{\bar{g}} \Phi_I R_{k,IJ} \Phi_J, \quad (7)$$

where  $I, J$  comprise internal indices and species of fields. For example, for the metric fluctuation  $\Phi_1 = h$  we have  $I = 1, \mu\nu$ . The regulator term in (7) has to be quadratic in the fluctuation field in order for the FRG flow equation to be of a particularly simple one-loop structure. Hence, the regulator contains a background field dependence with  $\sqrt{\bar{g}}$ . Moreover, it is chosen such that it suppresses low-momentum fluctuations in the path-integral, while high-momentum ones are integrated out. In gravity this again necessitates the specification of a metric, and hence also  $R_k$  depends on the background metric, e.g., via the covariant background Laplacian  $\Delta_{\bar{g}}$ . The explicit form of the regulators  $R_{k,IJ}$  used in the present work is given in App. D.

Within this framework  $\Gamma_k$  interpolates between the microscopic action for  $k \rightarrow \infty$  and the full quantum effective action for  $k \rightarrow 0$ . The effective action  $\Gamma_k[\bar{g}_{\mu\nu}, \Phi]$  obeys a one-loop flow equation, the Wetterich equation [83],

$$\partial_t \Gamma_k := k \partial_k \Gamma_k = \frac{1}{2} \text{Tr} \frac{1}{\Gamma_k^{(2)}[\bar{g}_{\mu\nu}, \Phi] + R_k} \partial_t R_k. \quad (8)$$

see also [84, 85]. In (8), the trace  $\text{Tr}$  includes a sum over internal indices and species of fields, including a negative sign for fermions, as well as a momentum-integration.  $\Gamma_k^{(2)} = \delta^2 \Gamma_k / \delta \Phi^2$  denotes the second functional derivatives of the effective action with respect to  $\Phi$ . This flow equation can be depicted as a 1-loop diagrammatic equation, as  $1/(\Gamma_k^{(2)} + R_k)$  corresponds to the full, field dependent propagator of the theory. The corresponding diagrams are not perturbative diagrams but rather fully non-perturbative depictions of derivatives of the above flow equation (8).

Quantum fluctuations generate all interactions which are compatible with the symmetries of the model. For practical purposes, it is necessary to truncate the space of all action functionals to a (typically) finite dimensional space. As our truncation, we choose (1). In the first part of this work, see Sec. III, we consider a truncation containing the first three lines in (1) and neglect all additional terms. In a canonical counting, all scalar-fermion interaction terms beyond this truncation are irrelevant. While residual interactions at an asymptotically safe fixed point alter the scaling properties of operators, the canonical dimensionality can still remain a useful ordering principle. In particular, if quantum fluctuations shift the critical exponents by anomalous contributions of  $\mathcal{O}(1)$ , then only a small number of couplings can be relevant. This reasoning has been demonstrated to hold in pure gravity within a truncation based on higher powers of the scalar curvature, [29]. Here, we adopt this

principle to motivate our truncation in the matter sector. More formally, our truncation can be understood as the leading order in a combined vertex- and derivative expansion, cf. App. B.

In the second part, cf. Sec. IV, we ask which of the higher-order couplings contained in  $\Gamma_{k,\text{ho}}[\bar{g}, \Phi]$  in (1) are induced by gravity. Specifically, these are the leading-order terms in a canonical counting, for which the only possible fixed point *must* be interacting. The vertices in the diagrams underlying their beta functions arise from the *kinetic* terms for scalars and fermions, and must respect the separate  $\mathbb{Z}_2$  symmetry in the scalar and chiral symmetry in the fermion kinetic terms (cf. last paragraph in Sec. II A). The canonically most relevant induced structures are of order  $p^3$  and read

$$\begin{aligned} \Gamma_{k,\text{ho}}[\bar{g}, \Phi] &= \Gamma_{k,\text{induced}} \\ &= i Z_\phi Z_\psi \bar{\mathcal{X}}_1 \int d^4 x \sqrt{\bar{g}} [(\partial_\mu \phi D^\nu \partial_\nu \phi) (\bar{\psi} \gamma^\mu \psi)] \\ &+ i Z_\phi Z_\psi \bar{\mathcal{X}}_2 \int d^4 x \sqrt{\bar{g}} [(\partial_\nu \phi D^\nu \partial_\mu \phi) (\bar{\psi} \gamma^\mu \psi)] \\ &+ i Z_\phi Z_\psi \bar{\mathcal{X}}_3 \int d^4 x \sqrt{\bar{g}} [(\partial_\nu \phi \partial_\mu \phi) (\bar{\psi} \gamma^\mu \nabla^\nu \psi)] \\ &+ i Z_\phi Z_\psi \bar{\mathcal{X}}_4 \int d^4 x \sqrt{\bar{g}} [(\partial_\nu \phi \partial^\nu \phi) (\bar{\psi} \gamma^\mu \nabla_\mu \psi)]. \quad (9) \end{aligned}$$

In App. B we give a more detailed discussion of our expansion in the matter and gravity sector. This also helps to understand the technical details as well as the systematics underlying the derivation of the  $\beta$ -functions of the matter couplings that are used for our analysis in Sec. III and Sec. IV.

### III. FIXED POINTS FOR THE YUKAWA COUPLING

In this section we analyze the UV-stability of the present Yukawa-gravity system, which serves as a toy model for the top-Yukawa sector of the Standard Model. It is a first step towards answering the question, whether asymptotically safe quantum gravity is compatible with a sizeable top-Yukawa coupling at the Planck scale  $M_{\text{Pl}}$ . This is required within the Standard Model without additional degrees of freedom up to  $M_{\text{Pl}}$ . Then, a perturbative evaluation is viable up to that scale, and yields  $y \approx 0.4/\sqrt{2}$  [72].

This is compatible with asymptotic safety within two physically distinct scenarios. In the first one, the Yukawa coupling features a UV-attractive fixed point, assuming that its value at the Planck scale lies within the basin of attraction of the fixed point. In the second scenario the Yukawa coupling becomes irrelevant at the fixed point. Then, its low-energy value, i.e., at momentum scales at or below the Planck scale, is a prediction of asymptotic safety. Disregarding the curvature of the critical surface,

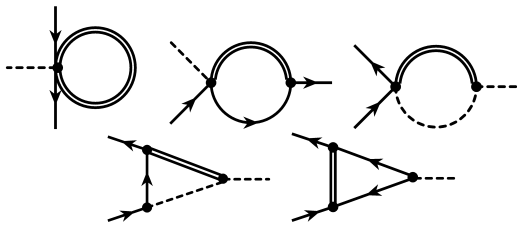


FIG. 1. Depicting metric propagators by a double line, scalars by a dashed line, and fermions by a directed line, we show the diagrams contributing to  $\beta_y$  that contain at least one metric propagator. All diagrams with  $n$  different internal propagators exist in  $n$  versions, with a regulator insertion on each of the  $n$  internal propagators. All contributions are  $\sim gy$ , and thus contribute directly to the critical exponent at a fixed point.

the fixed-point value would have to correspond to the value at the Planck scale.

### A. Results

We analyze the RG flow of the Yukawa coupling within the truncation specified by (1) with  $\Gamma_{k\text{ho}} = 0$ , cf. Fig. 1. The full result for the gravity-induced part is lengthy and thus presented in App. F. We recover the standard pure-matter contribution that agrees with FRG results in [52], such that

$$\beta_y = \frac{y}{2} (\eta_{\phi,0} + 2\eta_{\psi,0}) + \frac{y^3}{16\pi^2} \left( \frac{1 - \eta_{\psi}/5}{1 + \mu_{\phi}} + \frac{1 - \eta_{\phi}/6}{(1 + \mu_{\phi})^2} \right) + \beta_y^{\text{grav}}, \quad (10)$$

where  $\beta_y^{\text{grav}} \sim yg$  and  $\eta_{\Phi} = -\partial_t \ln Z_{\Phi}$ . In (10) we have introduced the dimensionless Newton coupling  $g/k^2 = G$ , and the dimensionless mass parameters  $\mu_h k^2 = -2\Lambda$ , as well as the dimensionless scalar mass  $\mu_{\phi} k^2 = m_{\phi}^2$ . Further details on the graviton propagator can be found in App. C. Note that we use that term in a loose way for the propagation of metric fluctuations. The latter are *not* restricted to small fluctuations around some background, and the ansatz therefore goes beyond the perturbative notion of a graviton propagator.

To compare to previous results, we note that if we fix the gauge parameters to  $\alpha = 0$  and  $\beta = 1$ , set the graviton mass parameter and all anomalous dimensions to zero such as to compare to [59] and [68], we come to agreement with the results obtained in [68],

$$\beta_y = \frac{y^3(2 + \mu_{\phi})}{16\pi^2(1 + \mu_{\phi})^2} + gy \frac{(29 - 2\mu_{\phi} + 5\mu_{\phi}^2)}{20\pi(1 + \mu_{\phi})^2}. \quad (11)$$

Note that in their notation  $\mu_{\phi} = 2\lambda_2$ . As the term  $y\bar{\psi}\psi\phi$  is only symmetric under a combined  $\mathbb{Z}_2$  transformation of the scalar,  $\phi \rightarrow -\phi$  and discrete chiral transformation of the fermions, while all other terms in the truncation

are invariant under these transformations separately, the RG flow of  $y$  must be proportional to  $y$ . Thus there is always a Gaussian fixed point  $y = 0$ . Therefore the asymptotically safe fixed point that has first been discovered in pure gravity in [2, 5] and has been shown to extend to a gravity-matter fixed point in minimally coupled truncations [55–58] trivially extends to the case with a Yukawa coupling. In particular, we can combine the Yukawa coupling with any truncation in the gravity-matter sector that already features a fixed point, and will find a trivial generalization of that fixed point. For definiteness, let us quote the results obtained in a vertex expansion for gravity and matter, first analyzed in [57] in the gauge  $\alpha = 0, \beta = 1$ , with

$$g_* \approx 0.55, \mu_{h,*} \approx -0.58, \eta_{h*} \approx 0.42, \eta_{c,*} \approx -1.58, y_* = 0, \mu_{\phi*} = 0, \eta_{\phi*} = \eta_{\phi,0*} = 0, \eta_{\psi*} \approx 0.07, \eta_{\psi,0*} \approx 0.72 \quad (12)$$

with a UV-irrelevant Yukawa coupling. We distinguish the anomalous dimensions from the definition of the vertex,  $\eta_{\psi/\phi,0}$ , from those arising from loop integrals, since our vertices are evaluated at vanishing momentum [57]. Note that corrections from Yukawa-diagrams to the matter anomalous dimensions  $\eta_{\phi/\psi}$  vanish at a fixed point with  $y = 0$ . Therefore the system in [57] does not change under the inclusion of a Gaussian Yukawa-coupling. Hence, by combining the results, we obtain the critical exponent of the Yukawa coupling,

$$\theta_y = -\left. \frac{\partial \beta_y}{\partial y} \right|_{y=0, g=g_*} \approx -2.33. \quad (13)$$

We compare this to the result that can be obtained in a hybrid background calculation, where the graviton anomalous dimension is distinguished from that of the background Newton coupling, but the graviton mass parameter is equated to the background cosmological constant, [55]. In that case, we obtain  $\theta_y = -0.06$ . While the sign is in agreement with (13), the absolute value differs significantly. We can trace that difference back to the background-approximation for the graviton mass parameter. In fact, using the fixed-point value for the Newton coupling and the anomalous dimensions from [55] and combining them with the mass parameter from [57], yields a critical exponent of  $\theta_y = -4.88$ .

### B. Gauge dependence

Next, we analyze the gauge-dependence of our result by varying the two gauge parameters  $\alpha$  and  $\beta$ . Note that in a consistent treatment we would substitute  $\alpha \rightarrow Z_{\alpha}\alpha, \beta \rightarrow Z_{\beta}\beta$  in the gauge fixing term (5), see App C. Here, we approximate  $Z_{\alpha} = 1 = Z_{\beta}$ .

First, we focus on the specific gravitational fixed-point values quoted in (12) in Figs. 2 and 3, which were obtained with  $\alpha = 0, \beta = 1$ , but which we extrapolate to other values of the gauge parameters. We observe poles

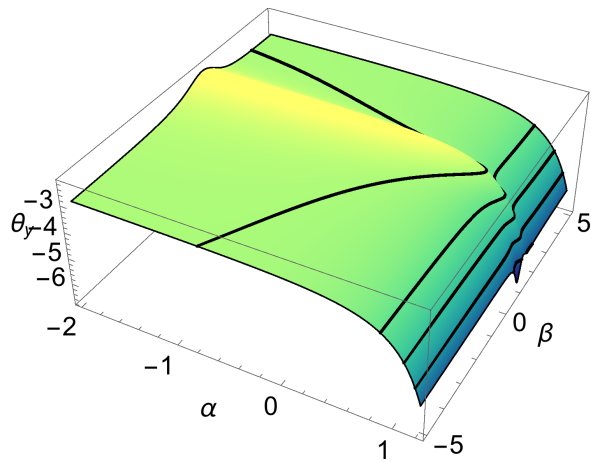


FIG. 2. We plot the critical exponent  $\theta_y$  for the fixed-point values given in (12) which were obtained with  $\alpha = 0$ ,  $\beta = 1$ . We extrapolate to other values of  $\alpha$  and  $\beta$  without adjusting the fixed-point values in the gravitational sector.

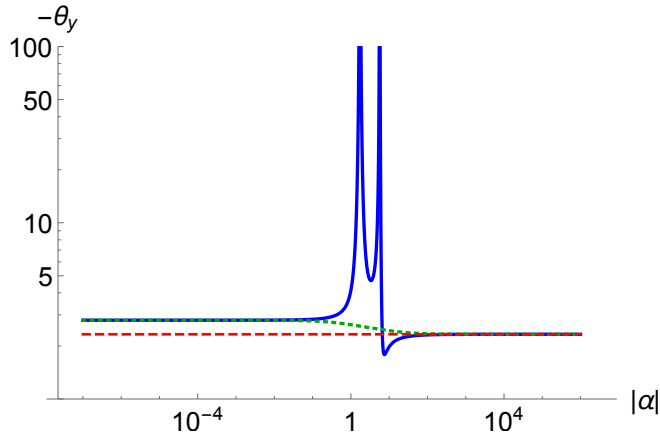


FIG. 3. We plot  $-\theta_y$  as a function of  $\alpha$  for the fixed-point values in (12). The blue thick curve is for positive  $\alpha$ , while the green dotted one is for negative  $\alpha$ . At large values, both reach the asymptotic limit  $\theta_y = -\frac{18}{25} - \frac{206838269}{40924800\pi}$  which is independent of  $\beta$ . The value of  $\theta_y$  at  $\alpha = 0$  depends on  $\beta$ , but is negative for all  $\beta$  for the values in (12).

at specific values of  $\alpha, \beta$ , which are induced by an incomplete gauge-fixing. Extrapolating the fixed-point values for the gravitational couplings that were obtained for the choice  $\alpha = 0$ ,  $\beta = 1$  into that region is inconsistent. We expect that in a complete study, in which the gravitational couplings, all anomalous dimensions and  $\theta_y$  are evaluated in a gauge-dependent way, these pole-structures disappear. It is reassuring to note that all values of  $\alpha$  and  $\beta$  excepting the poles lead to the same sign for the critical exponent,  $\theta_y < 0$ , cf. Fig. 3. Within the flow equation, positive and negative values of  $\alpha$  seem admissible, as both result in an invertible two-point function. On the other hand, choosing  $\alpha < 0$  flips the sign of the contribution of the vector mode to  $\beta_y$ . Within the path-integral,

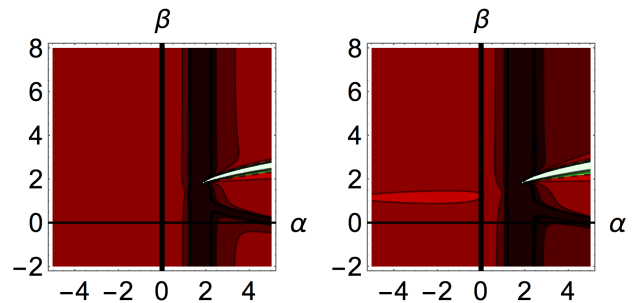


FIG. 4. We plot the critical exponent  $\theta_y$  as a function of the gauge-parameters  $\alpha$  (horizontally) and  $\beta$  (vertically). Green and lighter (red and darker) areas indicate positive (negative) values of  $\theta_y$  and thus a relevant (irrelevant) Yukawa coupling. Contours are drawn at  $-8, -6, -4, -2, 0, 2, 4, 6, 8$  and  $10$ . The black axis indicates the line along which the gauge-parameters take fixed point values at  $\alpha^* = 0$ . Additional parameters ( $g, \mu_h, \mu_\phi, \eta_h, \eta_\phi, \eta_\psi$ ) are set to the values from [57] (left panel), and from [55] with the fixed-point value for the graviton mass parameter taken from [57] (right panel).

only  $\alpha \geq 0$  naively corresponds to an implementation of the gauge-condition. For our choice of gravitational couplings, both signs of  $\alpha$  lead to a negative critical exponent for the Yukawa coupling, cf. Fig. 4. We observe a similar behavior if we use the fixed-point values from [55], combined with the fixed-point value  $\mu_{h*} \approx -0.58$  from [57], cf. Fig. 4. Resolving the background-approximation for the graviton mass parameter has a significant impact on the results, see upper left panel in Fig. 5: If the fixed-point value for the background cosmological constant is used for the graviton mass parameter, the sign of the critical exponent is not stable with respect to variations of the gauge. Note that in Fig. 5 we use fixed-point values obtained for the gauge  $\beta = 1 = \alpha$  away from that point. A more consistent study of the gauge dependence of our result should also include gauge-dependent gravitational fixed-point values. Nevertheless the strong gauge dependence could be interpreted as a hint that a resolution of the background-approximation is of particular importance for the graviton mass parameter, at least when matter fields are present.

For vanishing masses and anomalous dimensions the gravitational contribution to the beta function for the Yukawa coupling reduces to

$$\beta_y^{\text{grav}} = yg \frac{(5\alpha(5\beta^2 - 30\beta + 53) + 35\beta^2 - 258\beta + 339)}{20\pi(\beta - 3)^2}. \quad (14)$$

For this case, the dependence on the gauge-parameters is depicted in the lower right panel of Fig. 5. In (14) a pole occurs in the propagator, when the gauge-fixing condition (5) does not correspond to a proper gauge fixing, cf. Eq. (C4), as well as [40]. While a particular choice of the gauge parameters can lead to a change of the sign of the critical exponent, cf. Fig. 5, it seems to be induced by the pole in the propagator that arises from a bad choice

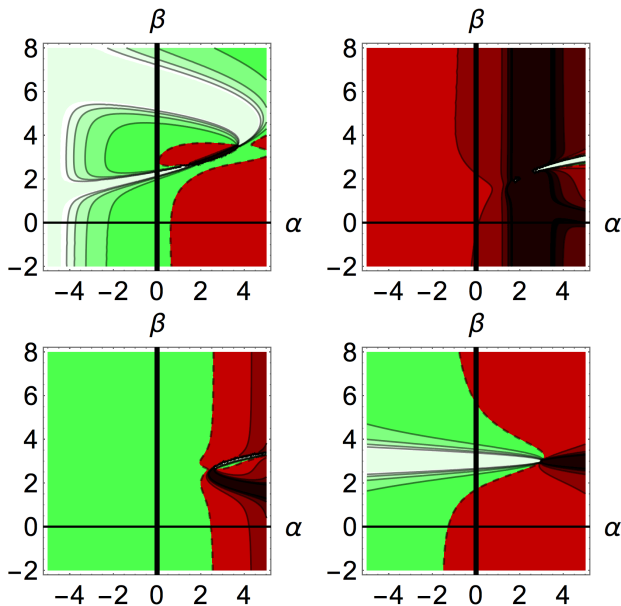


FIG. 5. We plot the critical exponent  $\theta_y$  as a function of the gauge-parameters  $\alpha$  (horizontally) and  $\beta$  (vertically). Green and lighter (red and darker) areas indicate positive (negative) values of  $\theta_y$  and thus a relevant (irrelevant) Yukawa coupling. Contours are drawn at  $-8, -6, -4, -2, 0, 2, 4, 6, 8$  and  $10$ . The dashed black curve highlights the crossing from negative to positive values. The black axis indicates the line along which the gauge-parameters take fixed point values at  $\alpha^* = 0$ . Additional parameters  $(g, \mu_h, \mu_\phi, \eta_h, \eta_\phi, \eta_\psi)$  are set to the values from [55] (upper left panel),  $(0.7, -0.42, 0, -2, 0, 0)$  (cf. [35], upper right panel),  $(0.55, -0.1, 0, -1, -1, 0)$  (lower left panel) and  $(0.55, 0, 0, 0, 0, 0)$  (lower right panel).

of gauge,  $\beta = 3$ .

Varying all gravitational parameters, we observe that some choices of  $\alpha, \beta$  can lead to a change in the sign of the critical exponent, which we tentatively consider an artifact.

### C. Stability & predictive power

In the last Section we have utilized results for the Newton coupling and the graviton mass parameter from

$$y_* = \pm \sqrt{\frac{\pi}{14(-6\eta_\psi - 5\eta_\phi + 60)}} \sqrt{g \left( \frac{24(231 - 41\eta_\psi)}{3 + 2\mu_h} + \frac{3(6888 - 869\eta_h)}{(3 + 2\mu_h)^2} - \frac{2800(6 - \eta_h)}{(1 + \mu_h)^2} \right) - 3360\pi(2\eta_{\psi,0} + \eta_{\phi,0})}. \quad (16)$$

We emphasize that large positive values of  $\mu_h$  are far from being accessible in state-of-the-art truncations in gravity. Nevertheless, they might be realized in extended truncations.

While matter interactions do not contribute directly to

[55, 57] for matter-gravity systems. These results were obtained in an approximation in which matter has no self-interactions at the UV fixed point.

Next, we consider effects beyond our truncation which will change the flow in the gravitational sector and the anomalous dimensions, but which do not couple directly into  $\beta_y$ . Thus we test how strongly any of the parameters  $g, \mu_h, \mu_\phi, \eta_h, \eta_c, \eta_\phi, \eta_\psi$  have to deviate from the results in (12) for the Yukawa coupling to become relevant.

As  $\beta_y^{\text{grav}} \sim yg$ , any positive fixed-point value for  $g$  will lead to the same sign of the critical exponent. Note that the restriction that the Newton coupling must be positive in the infrared precludes a negative fixed-point value, as the RG flow for  $g$  is  $\sim g$ , and therefore cannot cross the Gaussian fixed point that separates positive from negative values.

We then focus on the preferred choice of gauge  $\alpha = 0$ , which corresponds to an RG fixed point [86]. The latter holds, as the gauge-fixing condition is strictly imposed, which cannot be changed by the -finite- flow. Further, we choose  $\beta = \alpha$ , while noting that the choice  $\beta = 1, \alpha = 0$  does not lead to any qualitative differences in our results, cf. Sec. III. We observe that a large positive mass-parameter of the graviton – corresponding to a negative cosmological constant in a single-metric truncation or a negative level-2-cosmological constant in a “bi-metric” truncation – can change the sign of the critical exponent, cf. Fig. 6, as can negative anomalous dimensions for matter. For instance, setting  $\mu_\phi = 0$  leads to

$$\theta_y := -\frac{\partial \beta_y}{\partial y} \Big|_{y=0} = -\frac{1}{2}(\eta_{\phi,0} + 2\eta_{\psi,0}) + g \frac{231 - 41\eta_\psi}{280\pi(3 + 2\mu_h)} - \frac{g}{6720\pi} \left( \frac{2800(6 - \eta_h)}{(1 + \mu_h)^2} - 3 \frac{6888 + 869\eta_h}{(3 + 2\mu_h)^2} \right). \quad (15)$$

At large enough  $\mu_h$  and/or large negative  $\eta_{\phi/\psi}$ , the last line in (15) is suppressed, and the positive contribution dominates. In that case, two further fixed-point solutions are pulled from the complex plane onto the real axis. The non-Gaussian fixed-point values are given by

the pure-gravity parameters, they couple back into the matter anomalous dimensions  $\eta_{\phi/\psi}$ . Even for a vanishing Yukawa coupling, tadpole diagrams from matter 4-point interactions will contribute, cf. Sec. IV. The corresponding changes in the anomalous dimensions could present

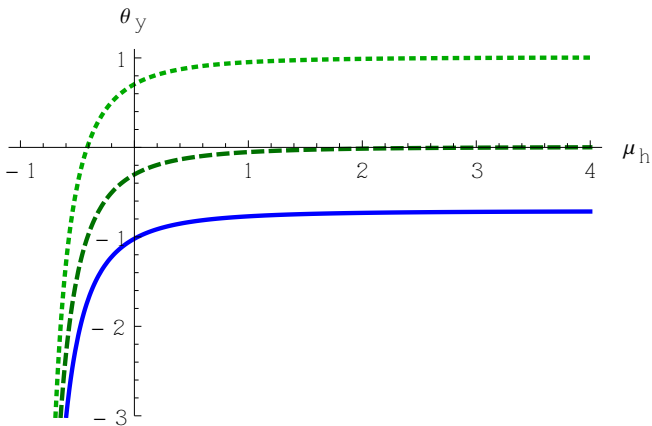


FIG. 6. We plot the gravitational contribution to the critical exponent of the Yukawa coupling divided by the Newton coupling, for gauge parameters  $\beta = \alpha = 0$ , and  $g^*, \eta_h^*$  from [57], as a function of the graviton mass parameter  $\mu_h$  for  $\eta_\psi = 0.07$  &  $\eta_{\psi,0} = 0.72$  (cf. (12); thick blue line),  $\eta_\psi = \eta_{\psi,0} = 0$  (dark green dashed line) and  $\eta_\psi = \eta_{\psi,0} = -1$  (light green dotted line).

another possible mechanism for pushing the Yukawa coupling into relevance, as negative (positive)  $\eta_{\phi/\psi}$  tend to make the Yukawa coupling more relevant (irrelevant), cf. Fig 6. Perturbing the fixed-point values from (12), the case of  $\eta_\psi = \eta_\phi = -1.411$  features a real fixed point (cf. (16)) at  $y_* \approx \sqrt{2} \cdot 0.4$  with critical exponents  $\theta_y = -0.01$ . This would enforce that particular value of the Yukawa coupling in the vicinity of the Planck scale, corresponding exactly to the value of the top-Yukawa coupling at that scale. Note that this scenario is contingent upon large negative values for the anomalous dimensions, which would require substantial changes from the results in (12). In general a scenario with additional non-Gaussian fixed points in the Yukawa coupling can be realized whenever there are negative contributions to the Yukawa  $\beta$ -function.

We conclude that in the present simple truncation the Yukawa coupling exhibits a Gaussian fixed point with irrelevant UV-behavior. We also observe that our calculation is compatible with a variety of approximations in the metric sector. For instance, within a single-metric approximation,  $g$  would correspond to the background-value for the Newton coupling, and  $\mu_h = -2\Lambda$ . As an example, we use fixed-point values from [40] with  $\eta_h = -2$ , which yield  $\theta_y = -1.44$  for  $g_* = 0.89$ ,  $\mu_h = -0.33$ ,  $\alpha = 0$ ,  $\beta = 1$ , and  $\theta_y = -1.97$  for  $g_* = 0.88$ ,  $\mu_h = -0.36$  for  $\beta = 0 = \alpha$  and finally  $\theta_y = -2.34$  for  $g_* = 0.72$ ,  $\mu_h = -0.32$  for  $\beta = 1 = \alpha$ . In a “bi-metric” calculation, the gravitational couplings entering the beta function for the Yukawa coupling would be those of the dynamical metric. Choosing  $g_* \approx 0.7$ ,  $\mu_h \approx -0.42$ ,  $\eta_h = -2$  and  $\alpha = 1, \beta = 1$ , as in [35] in fact leads to a critical exponent of  $\theta_y = -3.16$ . Thus, our conclusions on the critical exponent of the Yukawa coupling do not rely on specific assumption for the approximation in the gravitational sector, but hold

using fixed-point values from various studies in the literature.

The irrelevance of this coupling signals that its low-energy value can be predicted. This could open the door to an observational test of asymptotically safe quantum gravity, as the low-energy values of the Yukawa couplings in the Standard Model are known experimentally. Neglecting the curvature of the critical surface, the fixed point cannot be reached in the UV, unless the low-energy value of the coupling already equals the fixed-point value. We would thus conclude that at the Planck scale, where the joint matter-gravity RG flow sets in, the Yukawa coupling would already have to vanish in order for the RG trajectory to reach the fixed point. While this is close to the right value for the Yukawa couplings of the Higgs to the bottom and all lighter quarks and leptons, we know that the top-Yukawa coupling in the Standard Model is of the order  $y \approx 0.4/\sqrt{2}$  at the Planck scale. This might suggest that the fixed point that we have analyzed here is not one which is compatible with the properties of the Standard Model at low energies. Note however, that statements about quantum gravity effects on the running couplings of the Standard Model are also generically scheme-dependent, see, e.g., [61, 65, 87–91]. As couplings do not directly correspond to observable quantities, non-universality is not a problem. Still, it implies that only results obtained in the same scheme can be compared. Finally, here we only consider a toy model of the Yukawa sector, and have neglected additional matter fields of the Standard Model, which have to be included, e.g., along the lines of [92]. In summary, such a comparison requires further work in order to be dependable.

Moreover extensions of the truncation are clearly indicated: A reliable evaluation of the anomalous dimensions for the matter fields is critical to settle these questions. As has already been pointed out for scalar fields and fermions [66, 67], quantum gravity fluctuations induce further momentum-dependent interactions at the fixed point. These couple directly into the flow of the anomalous dimension, and are thus of critical importance for our study. This will entice us to consider in more detail, whether the above truncation already captures all important effects of quantum gravity on the Yukawa sector. As we will show in the next sections, it does not.

#### IV. GRAVITY-INDUCED MATTER INTERACTIONS

As has been pointed out for scalar and fermionic systems separately [66, 67, 69, 93], asymptotically safe quantum gravity induces non-vanishing matter self-interactions at the fixed point, cf. Fig. 7. Thus the only possible fixed points that exist for the joint matter-gravity system are necessarily non-Gaussian in some of the matter couplings. Clearly, the Yukawa coupling is not one of them, as all couplings with an odd number of matter fields can vanish. This scenario is as close as



FIG. 7. Mixed quartic diagrams generated by covariant kinetic terms in the flow equation. These diagrams are nonzero, even if all matter self-interactions are set to zero initially. They prevent the corresponding 2-scalar-2-fermion couplings from being able to reach asymptotic freedom.

possible to a fixed point that is Gaussian in the matter sector. Then, the first, genuinely gravity-induced couplings are the matter four-point vertices. Here we investigate the impact of the two-fermion–two-scalar couplings. The four-fermi, and four-scalar couplings have been discussed separately in gravity-fermion systems, [66, 69], and gravity-scalar systems, [67].

There are two main questions:

- Is there a fixed point in the matter-gravity system?
- Are canonically irrelevant couplings shifted into relevance at the joint fixed point?

Note that the first is a vital question since it is a necessary condition for the realization of asymptotic safety in a quantum theory of gravity combined with matter fields.

### A. Synopsis

In this section, we show that certain momentum-dependent scalar-fermion interactions *cannot* have a Gaussian fixed point in the presence of asymptotically safe gravity. In particular we show that the Gaussian matter fixed point for vanishing gravitational coupling  $g$  is shifted to an interacting one at finite  $g$ , called the shifted Gaussian fixed point (sGFP). Thus, asymptotically safe quantum gravity cannot be coupled to a fully asymptotically free matter system. At least a subset of the matter couplings must become asymptotically safe. This entails that the scaling dimensions of these couplings depart from canonical scaling. In fact, we observe that the canonically irrelevant scalar-fermion couplings will be pushed towards relevance.

Moreover, we find that for large enough gravitational coupling, the sGFP moves off into the complex plane. Then, the only remaining viable fixed points are fully interacting and exhibit a larger number of relevant directions.

Our main results are summarized in Fig. 12, where light grey dots mark a region where the shifted Gaussian fixed point does not exist. The fixed-point values obtained in [57] lie within the green region, where the shifted Gaussian fixed point exists.

### B. Induced two-fermion–two-scalar interactions

From here on, we work in the gauge  $\alpha = 0$  and  $\beta = 1$ . Including the covariant matter kinetic terms in the action automatically generates vertices with two matter fields and an arbitrary number of gravitons, i.e.,

$$S_{\psi,\text{kin}} = i \int d^4x \sqrt{g} (\bar{\psi} \gamma_\mu \nabla^\mu \psi) \quad (17)$$

$$\Rightarrow \begin{array}{c} \text{---} \\ \diagup \quad \diagdown \\ \text{---} \end{array} \quad \begin{array}{c} \text{---} \\ \diagdown \quad \diagup \\ \text{---} \end{array} \quad \dots \quad \begin{array}{c} \text{---} \\ \diagdown \quad \diagup \\ \text{---} \end{array}$$

$$S_{\phi,\text{kin}} = \frac{1}{2} \int d^4x \sqrt{g} (g^{\mu\nu} \partial_\mu \phi \partial_\nu \phi) \quad (18)$$

$$\Rightarrow \begin{array}{c} \text{---} \\ \diagdown \quad \diagup \\ \text{---} \end{array} \quad \begin{array}{c} \text{---} \\ \diagup \quad \diagdown \\ \text{---} \end{array} \quad \dots \quad \begin{array}{c} \text{---} \\ \diagdown \quad \diagup \\ \text{---} \end{array}$$

These vertices give rise to diagrams that induce higher order  $2s$ -point,  $2f$ -point and  $2s$ - $2f$ -point functions, where  $2s, 2f$  is the number of external scalar and fermion fields respectively. Couplings with an odd number of external fermions or scalars are not purely gravity-induced from the kinetic terms. We follow canonical power counting, and focus on the leading order terms in the corresponding expansion in the remainder of this section, which has  $s = f = 2$ . The fixed-point properties of the corresponding couplings is encoded in the four types of diagrams shown in Fig. 7. These diagrams are *non-vanishing, even if all matter self-interactions are set to zero*. Thus, if we switch off all matter self-interactions, but keep a finite gravitational coupling, the beta-functions of these quartic scalar-fermion couplings will be nonzero. Accordingly, there are scalar-fermion couplings which *cannot* vanish at a matter-gravity fixed point. This leads us to the gravity-induced higher order couplings already put down in (9). For further explanations about the tensor structures of these operators see App. G. For the sake of a fixed-point analysis it is convenient to introduce dimensionless couplings, to wit

$$\mathcal{X}_i = \bar{\mathcal{X}}_i k^4. \quad (19)$$

Inserting the definition (19) in (9) leads us to

$$\begin{aligned} \frac{\Gamma_{k\text{ induced}}}{i Z_\phi Z_\psi k^4} = & \left( \mathcal{X}_1 \int d^4x \sqrt{g} [(\partial_\mu \phi D^\nu \partial_\nu \phi) (\bar{\psi} \gamma^\mu \psi)] \right. \\ & + \mathcal{X}_2 \int d^4x \sqrt{g} [(\partial_\nu \phi D^\nu \partial_\mu \phi) (\bar{\psi} \gamma^\mu \psi)] \\ & + \mathcal{X}_3 \int d^4x \sqrt{g} [(\partial_\nu \phi \partial_\mu \phi) (\bar{\psi} \gamma^\mu \nabla^\nu \psi)] \\ & \left. + \mathcal{X}_4 \int d^4x \sqrt{g} [(\partial_\nu \phi \partial^\nu \phi) (\bar{\psi} \gamma^\mu \nabla_\mu \psi)] \right), \quad (20) \end{aligned}$$

where the flow of the left hand side can be easily projected on the couplings  $\mathcal{X}_i$ , see App G.

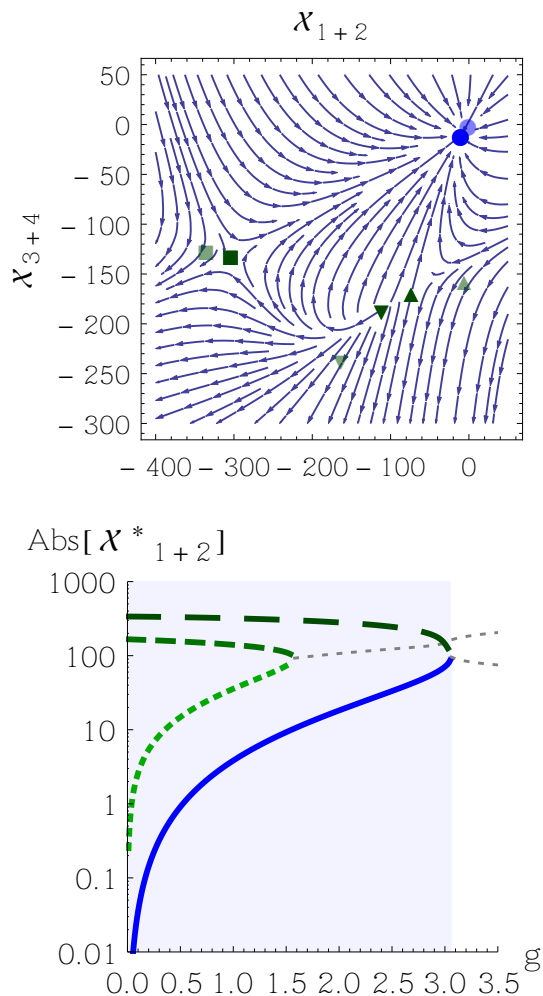


FIG. 8. Flow lines towards the UV for  $g = 1.5$  upper panel in the  $\mathcal{X}_{1+2}$ - $\mathcal{X}_{3+4}$ -space (all other matter couplings set to zero). The four fixed points sGFP, NGFP1, NGFP2 and NGFP4 are marked by a circle, up-triangle, down-triangle and square respectively. Lighter colored points mark the location of the fixed points at  $g = 0$ . Lower panel: Fixed-point values as a function of  $g$  for the sGFP (solid blue), NGFP1 (dotted), NGFP2 (dashed) and NGFP3 (wide-dashed). Real parts of complex fixed-point values are shown in light gray.

### C. Fixed-point shifts and annihilations in a simplified system

#### 1. Beta functions

In (20) there are two distinct classes of interactions:  $\mathcal{X}_{1,2}$  are independent of the momenta of the fermions, whereas  $\mathcal{X}_{3,4}$  are not. As a first step, we thus group them together into only two distinct couplings: We employ the projection rules specified in (G2) and (G3) to project onto  $\mathcal{X}_{1+2}$  and  $\mathcal{X}_{3+4}$ . This yields  $\beta$  functions for the combined couplings. The intriguing properties that we will observe in this simplified system persist within

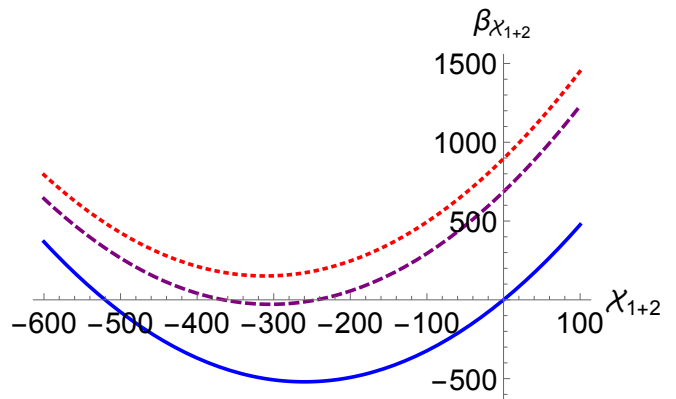


FIG. 9. We plot the beta-function for  $\mathcal{X}_{1+2}$  for  $\mathcal{X}_{3+4} = 0$  and vanishing anomalous dimensions and metric mass parameter for  $g = 0$  (blue thick line),  $g = 7$  (purple dashed line) and  $g = 8$  (red dotted line). The Gaussian fixed point at  $\mathcal{X}_{1+2} = 0$  only exists for  $g = 0$ , and then becomes shifted to an interacting fixed point at finite  $g$ , which annihilates with the second interacting fixed point at  $g \approx 7.2$ .

a more extended analysis, see Sec. IV D. For the sake of simplicity we have set the metric mass parameter and all anomalous dimensions to zero. The  $\beta$ -function for  $\mathcal{X}_{1+2}$  reads

$$\begin{aligned} \beta_{\mathcal{X}_{1+2}} = & 4\mathcal{X}_{1+2} + 14g^2 + \frac{37}{120\pi}g\mathcal{X}_{1+2} \\ & + \frac{17}{224\pi^2}\mathcal{X}_{1+2}^2 + \frac{25}{224\pi^2}\mathcal{X}_{1+2}\mathcal{X}_{3+4} - \frac{639}{560\pi}g\mathcal{X}_{3+4}, \end{aligned} \quad (21)$$

while the  $\beta$ -function for  $\mathcal{X}_{3+4}$  is given by

$$\begin{aligned} \beta_{\mathcal{X}_{3+4}} = & 4\mathcal{X}_{3+4} + 14g^2 - \frac{99}{80\pi}g\mathcal{X}_{3+4} \\ & + \frac{57}{224\pi^2}\mathcal{X}_{3+4}^2 - \frac{41}{224\pi^2}\mathcal{X}_{1+2}\mathcal{X}_{3+4} + \frac{17}{224\pi^2}\mathcal{X}_{1+2}^2. \end{aligned} \quad (22)$$

The key effect of gravity is encoded in the terms  $14g^2$  in Eqs. (21) and (22), which imply that no Gaussian fixed point in  $\mathcal{X}_{1+2}$  and  $\mathcal{X}_{3+4}$  can exist at finite  $g$ . A major result of ours is that as soon as metric fluctuations are switched on, the Gaussian fixed point is shifted to become interacting (cf. Fig. 8: lower panel). Accordingly, its scaling exponents deviate from the canonical value  $-4$ , and become less irrelevant, cf. Tab. I. At finite  $g$ , this fixed point is distinct from other possible interacting fixed points as its scaling exponents still reflect the canonical irrelevance of the two couplings.

#### 2. Fixed-point annihilations and excluded regions

At finite gravitational couplings  $g, \mu_h$ , the system shows an intriguing interplay of several fixed points,

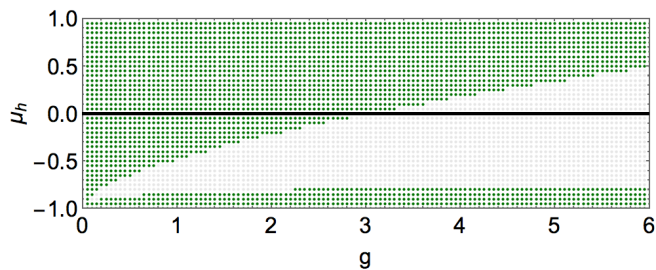


FIG. 10. Existence of the fully attractive sGFP in the simplified  $\mathcal{X}_{1+2}$ - $\mathcal{X}_{3+4}$ -truncation for different values of the gravity parameters  $(g, \mu_h)$  at vanishing anomalous dimensions. Darker green dots in the  $g, \mu_h$  plane mark existence regions while lighter gray dots indicate the loss of a fully attractive fixed point.

which can collide and annihilate. These are best understood starting from the gravity-free case: At  $g = 0$ , the system features four real fixed points, cf. Tab. I, one of which is the Gaussian fixed point. As a function of  $g$ , these fixed points move to different locations in the  $\mathcal{X}_1, \mathcal{X}_2$ -plane, cf. Fig. 8. At  $g = 2$ , two of the non-Gaussian fixed points have been driven to a collision by metric fluctuations and only the shifted Gaussian fixed point and one further fixed point still exist, cf. Tab. I.

$g$	$\mathcal{X}_{1+2}^*$	$\mathcal{X}_{3+4}^*$	$\theta_1$	$\theta_2$	
0	0	0	-4	-4	GFP
	0	-155.1	4	-2.25	NGFP1
	-166.5	-240.5	4	2.60	NGFP2
	-337.6	-124.1	4	-5.26	NGFP3
1	-3.84	-3.95	-3.49	-3.98	sGFP
	-35.7	-159.8	3.63	-1.40	NGFP1
	-140.0	-210.2	4.42	3.77	NGFP2
	-319.4	-128.4	3.77	-4.42	NGFP3
2	-18.2	-19.2	-2.63	-3.63	sGFP
	-280.9	-132.2	3.15	-3.14	NGFP3

TABLE I. Fixed-point values and critical exponents in the  $\mathcal{X}_{1+2}$ - $\mathcal{X}_{3+4}$ -truncation (all other matter couplings set to zero) for  $g = 0$ ,  $g = 1$  and  $g = 2$ , for vanishing graviton mass parameter and vanishing anomalous dimensions.

The effect of gravitational fluctuations becomes even more severe beyond  $g \approx 3.1$ , where all four fixed points have been driven to a collision. Within our truncation, no real fixed point exists beyond this critical value of  $g$ .

The same effect is already obvious from a truncation with  $\mathcal{X}_{3+4} = 0$ , cf. Fig. 9. As can be checked by evaluating the momentum-dependence of the right-hand side of the flow equation, our projection captures the momentum-dependence in this channel rather well. This might be interpreted as a sign that the fixed-point annihilation that we observe is not induced by neglecting higher-order momentum dependence in this truncation.

The effect of switching on the metric mass parameter  $\mu_h$  is opposite to a rising gravitational coupling  $g$  since the gravitational interaction strength is related to

the combination  $g/(1 + \mu_h)$ . Accordingly we observe the same collisions in the matter sector for decreasing  $\mu_h$ , in fact they occur along a line of  $g_{\text{crit.}}/(1 + \mu_{h,\text{crit.}})$ , cf. Fig. 10. Our simple truncation demonstrates our three main points:

- Asymptotically safe quantum gravity switches on certain matter interactions.
- Quantum-gravity fluctuations can lead to fixed-point annihilations in the matter sector.
- These fixed-point annihilations require the effective strength of gravitational interactions to exceed a critical value which is well beyond that reached in results in the literature, see, e.g., [35, 55, 69].

If the second point persists beyond our first explorative truncation, and does not prove to be a truncation artifact, it can impose a parameter restriction of asymptotic safety based on phenomenological viability. It is thus crucial to understand the system of induced interactions in more detail, to clarify whether asymptotically safe gravity is compatible with the existence of a Yukawa sector in Nature. In this spirit, we provide a first step by analyzing the full system in the next section.

#### D. Induced fixed-point interactions: the full system

##### 1. Shifted Gaussian fixed point and fixed-point annihilations

After the instructive, simplified analysis in the reduced system in the previous Section, we now take into account all two-fermion–two scalar interactions as put down in (20). To fully disentangle all tensor structures in the  $\mathcal{X}_i$  sector we now use a projection on all four couplings separately, cf. Eqs. (G6)-(G9). After projecting out the terms with three momenta, we choose a fully symmetric momentum configuration, cf. App. G. The resulting beta-functions are presented in App. H.

For vanishing Newton coupling,  $g = 0$ , the matter system exhibits 16 complex fixed points. In addition to the Gaussian fixed point five interacting fixed points are purely real and thus potentially physical. The values of all real fixed points and critical exponents can be found in App. I.

In a first step, we keep  $\mu_h = \eta_h = \eta_\phi = \eta_\psi = 0$  and only vary the gravitational interactions with  $g$ . In this process gravity not only shifts the six real fixed points (sGFP, NGFP1/2/3/4/5) of the pure matter system, cf. Fig. 11. It also pulls a pair of complex fixed points into the real plane (NUCFP1, NUCFP2) at  $g \approx 5.35$ , cf. Fig. 11, right panel.<sup>1</sup> If they persist beyond our truncation, these correspond to a new universality class of combined matter

<sup>1</sup> In fact, this generation of new universality classes when several interacting sectors are coupled to each other is a generic mech-

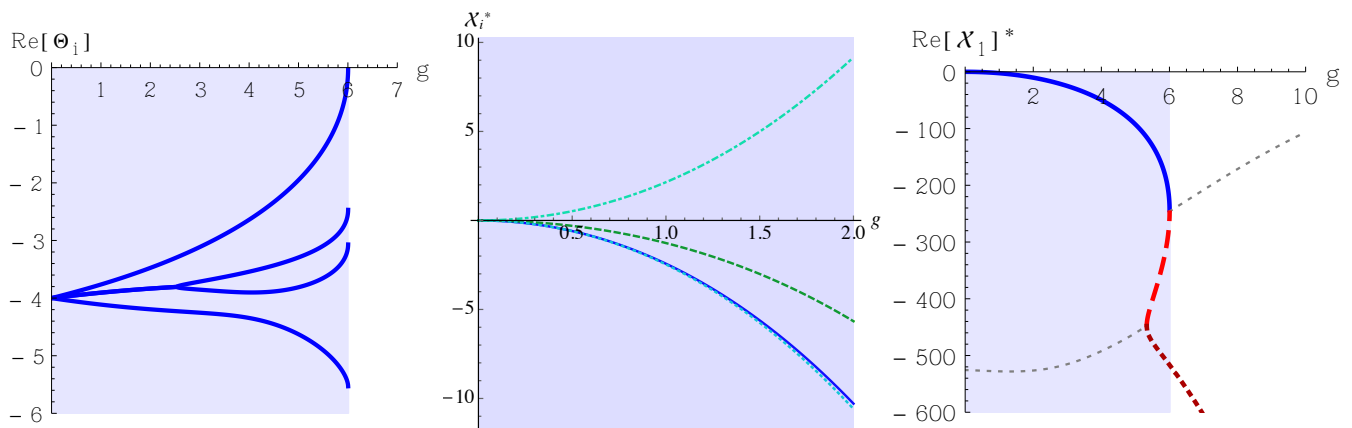


FIG. 11. Left-hand panel: Real parts of the critical exponents of the shifted Gaussian fixed point (sGFP) in the fully disentangled  $\mathcal{X}_i$ -truncation for growing  $0 < g < 7$ . The blue-shaded area marks the region where all fixed point coordinates are real. The fixed point collision at  $g \approx 6$  (cf. right-hand panel) is accompanied by a vanishing critical exponent. Middle panel: Change of fixed-point coordinates  $\mathcal{X}_i^*$  of the shifted Gaussian fixed point (sGFP) with growing  $0 < g < 2$  with  $\mathcal{X}_1^*$  (thick blue line),  $\mathcal{X}_2^*$  (dashed green line),  $\mathcal{X}_3^*$  (light blue, dotted line) and  $\mathcal{X}_4^*$  (turquoise dot-dashed line). Right-hand panel: As before (but now for  $0 < g < 10$ ). Now the  $\mathcal{X}_1$  coordinate is shown for the sGFP (blue), NUCFP1 (red, dashed) and NUCFP2 (darker red, dotted), featuring both the emergence of the NUCFPs as well as the collision of sGFP and NUCFP1. Before emergence and after the collision the real parts of the fixed point coordinates are drawn in thin gray dotted lines.

and gravity, which is not present in either system alone and would emerge at finite interaction strength.

The shifted Gaussian fixed point (sGFP) remains UV repulsive in all four directions but becomes non-Gaussian when gravity is switched on, cf. Fig. 11. The gravitational contribution to the scaling dimensionality of the  $\mathcal{X}_i$  is positive for the first three of these couplings. Accordingly, they are shifted towards relevance. At  $g \approx 6$ , the shifted Gaussian fixed point collides with one of the other interacting fixed points, and moves off into the complex plane. As expected, this fixed-point collision is accompanied by a change in sign in one of the critical exponents, cf. Fig. 11, left panel. Thus gravity might not only deform the universality class of an asymptotically free matter fixed point, but might even completely destroy it. In the range of values for  $g$  where the shifted Gaussian fixed point does not exist, several other interacting fixed points lie at real coordinates. These provide possible universality classes for the matter system coupled to gravity. As the presence of additional interacting fixed points is a difference to the simpler truncation analyzed in Sec. IV C, it is not clear whether these are truncation artifacts. Our results exemplify, that the regime of very strong gravitational coupling could correspond to a setting, where the UV completion for the Standard Model coupled to gravity might be one which is fully non-Gaussian, and

which is actually *not* a quantum-gravity deformation of an asymptotically free fixed point.

## 2. Allowed gravitational parameter space

The effective gravitational interaction strength is related to the combination  $g/(1+\mu_h)$ , and thus grows with increasing  $g$  and decreasing  $\mu_h$ . Thus at a very large mass parameter, the shifted Gaussian fixed point is nearly Gaussian. As a function of decreasing mass parameter, it then undergoes the same type of collisions as it does as a function of increasing  $g$ . We thus conclude that the shifted Gaussian fixed point does not exist in all regions of the  $g\mu_h$ -plane within our truncation, cf. Fig. 12. If we assume that a phenomenologically viable fixed point has to be the shifted Gaussian one, in order to smoothly connect to the perturbative behavior of the Standard Model in the vicinity of the Planck scale, the gray region in Fig. 12 is excluded from the viable gravitational parameter space in our truncation.

Comparing these results to the simpler truncation in Section IV C, we observe that the region in which the shifted Gaussian fixed point is complex remains quantitatively similar and persists. Whether this trend persists under further extensions of the truncation is an important question for future studies.

Matter anomalous dimensions shift the areas of existence of the shifted GFP as they shift the critical exponents and therefore also the locations where these cross zero. Interestingly, the fixed point values of the non-interacting matter-gravity sector [57] fall into a regime

anism. It has also been observed in three-dimensional scalar theories, when several scalar sectors are coupled to each other [94, 95], as well as in four-dimensional gauge theories, where semi-simple gauge groups exhibit a new, fully interacting fixed point that does not exist for a simple gauge group [96].

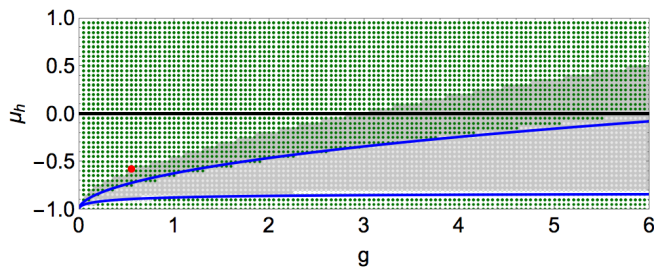


FIG. 12. Existence of a fully attractive fixed point corresponding to the shifted Gaussian fixed point in the fully disentangled  $\mathcal{X}_i$ -truncation for different values of the gravity parameters  $(g, \mu_h)$  and vanishing anomalous dimensions. Darker green dots in the  $g, \mu_h$  plane mark existence regions. For the gravitational fixed point values  $g_* \approx 0.55$  and  $\mu_{h,*} \approx -0.58$  (red dot) from [57] an interacting matter fixed point with four irrelevant directions exists. These fixed-point values have been obtained for non-vanishing anomalous dimensions. Given the anomalous dimensions from [57] the combined fixed point still persists. The dark-shaded grey area is the region where no shifted GFP exists in the simpler truncation, cf. Fig. 10. Inbetween the two thick blue lines, no shifted GFP exists in the simplest truncation, cf. Fig. 9. We observe qualitative agreement between the different approximations. Surprisingly, the simplest truncation with only one coupling even agrees with our most elaborate truncation with four distinct couplings at a quantitative level.

of gravitational strength where the shifted GFP of the  $\mathcal{X}$ -sector exists (cf. App. I), with

$$\begin{aligned} \mathcal{X}_1^* &= -8.64, \quad \mathcal{X}_2^* = -4.70, \quad \mathcal{X}_3^* = -8.55, \quad \mathcal{X}_4^* = 7.78, \\ \theta_1 &= -4.64, \quad \theta_2 = -4.31, \quad \theta_3 = -4.23, \quad \theta_4 = -4.09. \end{aligned} \quad (23)$$

cf. Fig. 12. Note that these values will be modified in a combination of the study in [57] with our truncation, as the  $\mathcal{X}_i$ -interactions alter the matter anomalous dimensions. As in Sec. III C, large negative matter anomalous dimensions can qualitatively alter our results. If, e.g.,  $\eta_\psi + \eta_\phi \lesssim -2.5$  the shifted Gaussian fixed point disappears. It is therefore crucial to quantify shifts in the matter anomalous dimensions due to the induced matter interactions. If such large shifts are indeed observed, truncations should include these interactions, even though they are of higher order according to our ordering principle of canonical dimensionality.

Combining the two aspects of the Yukawa sector that we have analyzed, we observe that the  $\mathcal{X}_i$  cannot couple directly into the flow of the Yukawa coupling, due to their derivative structure. Thus, a truncation including  $y, \mathcal{X}_i$  still features the Gaussian fixed point for  $y$ . This fixed point can be combined with any of the fixed points in the  $\mathcal{X}_i$  sector, which remain unaltered by the inclusion of  $y$ . On the other hand, a more extended truncation, including momentum-dependent Yukawa couplings, as well as two-fermion–two-scalar couplings with a lower power of momenta could feature contributions of these new couplings to both  $\beta_y$  as well as  $\beta_{\mathcal{X}_i}$ .

## V. CONCLUSIONS AND OUTLOOK

As a step towards a unification of the Standard Model with quantum gravity within the paradigm of asymptotic safety, we have performed an extensive analysis of a Yukawa system. Our model consists of a Dirac fermion and a scalar, coupled to asymptotically safe quantum gravity. The fixed-point structure of our model is determined by two major quantum-gravity effects on the matter sector:

1. Quantum-gravity fluctuations generate a correction to the quantum scaling of matter operators.
2. Quantum-gravity fluctuations induce non-zero matter self interactions, triggering a departure from asymptotic freedom in the matter sector.

The first property is of particular interest in a scenario where no additional matter degrees of freedom exist up to the Planck scale. There, a direct connection can be established between low-energy values of the Standard Model couplings, and the properties of a joint matter-gravity fixed point. In particular, the low-energy values of irrelevant couplings can be predicted, thus potentially enabling observational tests of the quantum-gravity regime. Our studies suggest that the Yukawa coupling could be used to bridge the gap between experimentally accessible scales and the Planck scale: In the UV, the Yukawa coupling in our toy model features a UV-repulsive fixed point at zero for most of the gravitational parameter space. This implies that it must already be very close to zero at the Planck scale. This condition is actually realized in Nature for the Yukawa couplings of the lighter leptons of the Standard Model. However the top Yukawa coupling is sizable at the Planck scale, which would probably prevent it from reaching a fixed point at zero in the far UV.

Within our toy model, there is a small region of parameter space for which the Yukawa coupling becomes relevant. Simultaneously, an interacting fixed point at which it is irrelevant is generated. If extended truncations feature a similar fixed point, a scenario is conceivable, in which the observed value of the top-Yukawa coupling is in fact a consequence of asymptotic safety.

For the Yukawa sector, the second major quantum-gravity effect is manifest in newly generated, momentum-dependent interactions. The lowest order gravity-induced interactions between fermions and scalars are two-fermion–two-scalar interactions with couplings  $\mathcal{X}_i$ . At vanishing gravitational coupling, the system features a non-interacting, Gaussian fixed point. Then, switching on quantum gravity fluctuations, the Gaussian matter fixed point is shifted, becoming an interacting fixed point which we call shifted Gaussian fixed point. In an extended truncation, we thus find only interacting fixed points for the  $\mathcal{X}_i$ , while the Yukawa coupling  $y$  is zero at that fixed point. Thus, the only viable matter-gravity fixed point appears to be one which is asymptotically safe, rather than asymptotically free, at least for a subsector of matter self-interactions. Unlike other interacting fixed points

of the matter system, the shifted Gaussian fixed point shows scaling exponents similar to the canonical ones, at least in the weak-gravity regime.

We have demonstrated that the model is dominated by an intriguing interplay of several fixed points at large values of the gravitational coupling. At a critical value of the gravitational coupling strength, one of these interacting fixed points collides with the shifted Gaussian fixed point. Subsequently, they disappear into the complex plane. Thus, the shifted Gaussian fixed point ceases to exist for larger values of the effective gravitational coupling. In fact, gravitational fixed-point values from recent studies lie within the regime allowing a shifted Gaussian fixed point, cf. Fig. 12 which summarizes our main results. Crucially, extending our truncation leads to quantitatively similar results on the allowed gravitational parameter space, cf. Fig. 12.

Our results highlight that even though the canonical dimensionality of the momentum-dependent matter interactions is irrelevant, they might nevertheless play a pivotal role in the dynamics of an asymptotically safe matter-gravity system. We conclude that quantum gravity could have a significant impact on the properties of the matter sector in the UV, and might even require a UV completion that deviates considerably from a shifted Gaussian fixed point and the associated near-canonical power counting. In order for this scenario to be realized, gravitational couplings must exceed a critical strength, which lies beyond that observed in the literature, see, e.g., [35, 55, 69]. Thus, truncations that neglect gravity-induced matter self interactions, and therefore discover a free fixed point in the matter sector might potentially not capture the properties of a matter-gravity fixed point at a qualitative level: If the joint matter-gravity fixed point is not the shifted Gaussian one, then the scaling exponents in the matter sector will be rather different from those at a Gaussian matter fixed point.

As one of our main results, we find that a shifted Gaussian fixed point with irrelevant fermion-scalar interactions and an irrelevant Yukawa coupling exists at gravitational fixed-point values from recent studies.

### A. Outlook

Our study also clearly indicates the need for extended truncations in the matter sector. In the future, we will extend our current study to include further matter interaction terms that have an impact on the scaling dimension of the Yukawa coupling and on the induced matter-interactions. A major missing piece of this puzzle are four-fermion interactions, which have been shown to feature only interacting fixed points under the effect of asymptotically safe quantum gravity [66, 69]. They feed back into the beta-functions in our system. Further, momentum-dependent self-interactions of scalars and fermion-scalar interactions will alter the value of the matter anomalous dimensions. As has been discussed in

Section IV, including dynamical anomalous dimensions is a critical step towards a quantitative control of the system.

It should be stressed that within asymptotically safe quantum gravity, the Einstein-Hilbert action is not the complete fixed-point action for gravity. Just as quantum fluctuations induce further matter interactions, higher-order terms, such as, e.g., curvature-squared terms, are also present. In particular, a subset of these corresponds to relevant couplings at a pure-gravity fixed point. Testing the impact of these terms on the matter sector is an important bit of the puzzle that we hope to come back to in the future.

On the phenomenological side, the quantum-gravity-generated fermion-scalar interactions could be of interest in the context of Higgs portals to fermionic dark matter, see, e.g., [97]: Asymptotically safe quantum gravity, according to our studies, contains a generic mechanism to couple dark sectors, e.g., additional scalars and fermions, to a scalar such as the Higgs. This coupling might therefore provide a basis for a possible connection of asymptotic safety to dark matter phenomenology.

### Acknowledgements

We thank Masatoshi Yamada for helpful discussions on [68]. We also thank Omar Zanusso and Manuel Reichert, Tobias Henz for discussions as well as Anton Cyrol, Mario Mitter, Andreas Rodigast and Tobias Denz for the (co-) development of the automated algebraic tools used in this computation [98–100]. This work is supported by EMMI and by ERC-AdG-290623. The work of A.E. is supported by an Imperial College Junior Research Fellowship.

## Appendix A: Background independence

The classical action of the present matter-gravity theory is given by the first three lines in (1) with  $Z_\Phi = 1$ , and the Einstein-Hilbert action, (4). This action is a function of a single metric field  $g$  and consequently, does not depend on the choice of the background metric  $\bar{g}$ . This statement generalizes to expectation values of diffeomorphism invariant operators for any quantized matter-gravity theory, based on a microscopic action that depends on a single metric. In turn, for diffeomorphism-variant correlation functions such as those of the metric fluctuations  $h$ , diffeomorphism invariance and background independence translate into non-trivial Slavnov-Taylor identities (STIs) and Nielsen identities (or split Ward identities), that depend on the background metric. This leads to the counter-intuitive situation, that any diffeomorphism-invariant and background-independent approximation to the fluctuation dynamics breaks the underlying diffeomorphism invariance and background independence of the theory. For further discussions see [36, 42, 57].

In the present setting with an additional regulator term (cf. App. D for a discussion of the employed regulators), the STIs turn into mSTIs and modified Nielsen identities (split Ward identities), see, e.g., [9, 16, 19, 20, 39, 44, 65, 78, 86, 101–104]. Importantly, regulator modifications scale with the cutoff  $k$  and are hence potentially dominant, in particular for the UV-relevant parameters. This makes the distinction between background and fluctuation quantities crucial. The flow of both, background and fluctuation correlations is generated by closed flow equations of the fluctuation propagator and vertices. In turn, only the background field effective action  $\Gamma_{k=0}[g; \tilde{\Phi} = \Phi = (0, 0, 0, \psi, \bar{\psi}, \phi)]$  is diffeomorphism invariant, background-independent and relates directly to S-matrix elements of the theory. By this reasoning – in order to compute diffeomorphism invariant and background-independent observables – we first have to solve the dynamical, closed system of fluctuation correlation functions  $\Gamma^{(n)}$  and use the latter in the flow of  $\Gamma_{k=0}[g; \tilde{\Phi}]$ .

## Appendix B: Expansion scheme

The vertex expansion reads

$$\Gamma_k[\bar{g}, \Phi] = \sum_n \frac{1}{n!} \Gamma^{(n)}[\bar{g}, 0] \Phi^n, \quad (\text{B1})$$

and requires the choice of a specific metric and matter background  $(\bar{g}, \Phi)$  as an expansion point. We choose  $\Phi = 0$ , which is a saddle point or minimum of the matter part of the effective action. A good physical choice for the metric background is a solution of the gravity equation of motion, which however complicates the computations considerably. Instead we choose a flat background,

$$\bar{g}_{\mu\nu} = \delta_{\mu\nu} \quad (\text{B2})$$

with a flat Euclidean metric. We emphasize that it is not necessary to choose a solution of the equations of motion,  $\bar{g}_{\text{EoM}}, \bar{\Phi}_{\text{EoM}}$  as the expansion point. It is expected, though, that such a choice  $\bar{g}_{\text{EoM}}, \bar{\Phi}_{\text{EoM}}$  leads to a more rapid convergence of the vertex expansion.

In the present work we use the lowest order of the vertex expansion in the matter sector to access low-order  $n$ -point functions. The related effective matter-gravity action underlying our results in Sec. III is summarized in the first three lines of (1) and amounts to  $\Gamma_{k,\text{ho}} = 0$ . This approximation also features an additional derivative expansion, as no higher momentum-dependences and additional tensor structures are considered. In its lowest order this leaves us with the scale-dependent Yukawa coupling  $y$ . Additionally, wave-function renormalizations  $Z_{\phi/\psi}$  are included. At the next order in our expansion scheme, these would be upgraded to field-dependent wave-function renormalizations. In this work, we neglect additional terms in the purely scalar sector which are

canonically relevant/ marginal, as they do not directly impact  $\theta_y$ , which is the main physics question we focus on.

In Sec. IV, we consider two-fermion–two-scalar interactions, induced by gravity. These interactions give rise to additional terms in the effective action,  $\Gamma_{k,\text{induced}}$  that are part of the higher order terms in  $\Gamma_{k,\text{ho}}$ . From the class of all gravity-induced interactions, these are the lowest-order terms in a combined derivative- and vertex expansion, i.e., they are those with the least irrelevant canonical dimensionality. Following a canonical counting, lower-order scalar-fermion interactions exist; however, these are not induced by gravity fluctuations directly. On the other hand, once gravity fluctuations switch on the  $\mathcal{X}_i$  interactions, these can induce further matter interactions, e.g., through tadpole diagrams. This backcoupling of quantum-gravity induced interactions will be the subject of a future work.

Finally, by using a metric split, cf.(3), in the matter part of the effective action (cf. (1)) we have identified all matter couplings to gravity with a single Newton coupling  $\sqrt{G}$ . Typically, such a universality holds for the first two non-vanishing perturbative coefficients of the  $\beta$ -function of a dimensionless coupling in a mass-independent renormalization scheme. None of the above hold in the current case. Instead, it is expected that all the gravity couplings run differently due to the missing universality as well as due to the regulator-induced modifications of the mSTIs. The respective modifications are either of higher order in the gravity fluctuation  $h$ , as well as higher order in derivatives.

Our computations rely on automated algebraic manipulation tools. For setting up the truncation as well as deriving the vertices and diagrams we use the Mathematica package TARDIS [100]. When calculating the traces of these diagrams we rely on the FormTracer package [98, 99].

## Appendix C: Gravity expansion

The above Section B summarizes our expansion scheme in the matter sector of the theory. For the fixed point analysis we also need the metric propagator as well as the Newton coupling in a flat background. Given the expansion in powers of the fluctuating graviton  $h$ , this is naturally augmented with results in the same expansion scheme for the gravity correlations put forward in [24, 36, 42, 57, 69], or with mixed approaches [28, 55, 58]. Equivalently, the same information can be encoded in an approach featuring the background metric as well as the full metric, [16, 19, 20, 35]. Note that our results for the matter sector can be combined with different approximation schemes in the gravity sector, as they simply use the gravitational couplings  $g, \mu_h$  and  $\eta_h$  as input parameters.

We adopt the linear split (cf. (3)) in the Einstein-Hilbert action (cf. (4)) in the spirit of the present combined vertex and derivative expansion, and drop higher

order terms. Full consistency of the present expansion scheme as a derivative expansion then also requires  $\alpha \rightarrow Z_\alpha \alpha$ ,  $\beta \rightarrow Z_\beta \beta$  in the gauge fixing term (5). With these cutoff dependences the quadratic part of the pure gravity effective action reads

$$\begin{aligned} \Gamma_{k, \text{grav}}^{(h,h)\mu\nu\rho\sigma} h_{\mu\nu} h_{\rho\sigma} &= \frac{Z_h}{64\pi} \int \frac{d^4 p}{(2\pi)^4} h_{\mu\nu}(p) h_{\rho\sigma}(-p) \\ &\times \left[ (\mu_h k^2 + p^2) g^{\mu(\rho} g^{\sigma)\nu} - (\mu_h k^2 + 2p^2) g^{\mu\nu} g^{\rho\sigma} \right. \\ &+ 2(g^{\mu\nu} p^\rho p^\sigma + g^{\rho\sigma} p^\mu p^\nu) - g^{\mu(\rho} p^{\sigma)} p^\nu - g^{\nu(\rho} p^{\sigma)} p^\mu \\ &- \frac{1}{Z_\alpha} \left( \frac{1 + Z_\beta \beta}{\alpha} (g^{\mu\nu} p^\rho p^\sigma + g^{\rho\sigma} p^\mu p^\nu) \right. \\ &\left. \left. + \frac{1}{\alpha} (g^{\mu(\rho} p^{\sigma)} p^\nu - g^{\nu(\rho} p^{\sigma)} p^\mu) + \frac{(1 + Z_\beta \beta)^2}{4\alpha} p^2 g^{\mu\nu} g^{\rho\sigma} \right) \right]. \end{aligned} \quad (\text{C1})$$

The present approximation is based on a common approximation on the mSTI in gauge theories, leading to a diffeomorphism-invariant representation with multiplicative wave function and coupling renormalizations. In this work it is induced by the truncation in (cf. (1)) with linear split (cf. (3)) and by using diffeomorphism-invariant terms in the effective action before substituting (3). This leads to a uniform wave function renormalization  $Z_h$  for all York decomposed components of the graviton propagator (cf. line 2 & 3 in (C1)), except for the gauge fixing terms (cf. last two lines in (C1)). The York decomposition reads

$$h_{\mu\nu} = h_{\mu\nu}^{\text{TT}} + 2\bar{D}_{(\mu} v_{\nu)} + \left( 2\bar{D}_{(\mu} \bar{D}_{\nu)} - \frac{1}{2} \bar{g}_{\mu\nu} \bar{D}^2 \right) \sigma + \frac{1}{4} \bar{g}_{\mu\nu} h, \quad (\text{C2})$$

with  $\bar{D}^\mu h_{\mu\nu}^{\text{TT}} = 0$ ,  $h_\mu^{\mu\text{TT}} = 0$ ,  $h_\mu^\mu = h$  and  $\bar{D}^\nu v_\nu = 0$ . In the gravity results used here  $Z_h$  is obtained from the traceless transverse part of the inverse propagator,  $Z_h = Z_{h, \text{TT}}$ .

Moreover, the related approximation of the mSTI leads to

$$Z_\alpha = Z_h, \quad Z_\beta = 1, \quad (\text{C3})$$

for the longitudinal directions singled out by the gauge condition in (5). For the sake of simplicity we have used the additional approximation  $Z_\alpha = 1$  for the results shown in this work. We have checked that the results do not differ significantly from the consistent choice (C3).

The respective results for gravity in the literature are mostly obtained in very few gauge choices, singled out by conceptual or technical reasons. For instance, the harmonic gauges,  $\beta = 1$ , or the Feynman gauge,  $\alpha = \beta = 1$ , lead to considerable technical simplifications. However, none of these gauges persists during the flow

for  $\alpha \neq 0$  beyond the current, classical, approximation to the mSTIs. In turn,  $\alpha = 0$  is a fixed point of the FRG flow, as the flow of  $1/\alpha$  is finite, see [86]. In terms of convergence of the current expansion in the gauge fixing sector of the theory this singles out the line  $(\alpha, \beta) = (0, \beta)$  as the most stable one.

The choice of  $\beta$  also rotates the physical mode in the scalar sector from pure trace-mode ( $\beta \rightarrow 0$ ) into pure  $\sigma$ -mode (see Eq. (21) in [40]). Inverting the scalar projection of the 2-point function onto the scalar York-sector  $\Gamma_{k, \text{grav}, (\sigma h)}^{(2)}[\Phi]$ , the corresponding part of the metric propagator is given by

$$\begin{aligned} \Gamma_{k, \text{grav}, (\sigma h)}^{(2)-1} &= \frac{64\pi G}{4\alpha\mu_h^2 + 2p^2(2\alpha - \beta^2 + 3)\mu_h + (\beta - 3)^2 p^4} \times \\ &\times \begin{pmatrix} p^2(\alpha - 3) - 2\alpha\mu_h & \sqrt{3}p^2(\alpha - \beta) \\ \sqrt{3}p^2(\alpha - \beta) & (3\alpha - \beta^2)p^2 + 2\alpha\mu_h \end{pmatrix}. \end{aligned} \quad (\text{C4})$$

This equation already shows that for  $\beta = 3$  the gauge-fixing is incomplete. In terms of RG-flows also the gauge-parameters should in fact be regarded as running quantities (directions in theory space). This viewpoint favors  $\alpha^* = 0$  (Landau-limit) as a UV-fixed point of the RG-flow [86].

Finally concerning the gauge-dependence of flows in the matter sector, e.g., the Yukawa coupling, it is interesting to observe that they only enter via the metric propagator or its regularized version

$$\begin{aligned} &\left( \Gamma_k^{(2)}[\bar{g}_{\mu\nu}, \Phi] + R_k \right)^{-1} \partial_t R_k \left( \Gamma_k^{(2)}[\bar{g}_{\mu\nu}, \Phi] + R_k \right)^{-1} \\ &= \frac{1}{((\beta - 3)^2 + 2\mu_h(2\alpha - \beta^2 + 2\alpha\mu_h + 3))^2} \times \\ &\times \frac{1}{(\mu_h + 1)^2} \frac{1}{(\alpha\mu_h + 1)^2} \times \text{analytic}. \end{aligned} \quad (\text{C5})$$

Since in all diagrams in Fig. 1 there is precisely one -possibly regulated- metric propagator, the gauge-pole structure of the Yukawa  $\beta$ -function is at most given by the above regulated propagator poles.

Indeed all gauge poles as well as poles in  $\mu_h$  are lifted when dividing (F1) by the pole structure given in (C5).

## Appendix D: Optimized regulators

For the explicit computations in the flat background we employ the Litim or flat cutoff [105, 106] in momentum space for the matter degrees of freedom,

$$R_{k, \phi}(p) = Z_\phi p^2 r_\phi(x), \quad R_{k, \psi}(p) = Z_\psi \not{p} r_\psi(x) \quad (\text{D1})$$

with  $x = p^2/k^2$ . The shape functions for bosons and fermions take the form

$$r_\phi(x) = (x - 1)\theta(1 - x), \quad r_\psi(x) = (\sqrt{x} - 1)\theta(1 - x), \quad (\text{D2})$$

The graviton propagator that enters the diagrams for the matter wave function renormalizations and the Yukawa coupling is represented in the York decomposition. The regulator used for all modes in the York decomposition (cf. (C2)) is the bosonic one in (D1), where  $Z_\phi p^2$  is substituted by the full kinetic factor that can be read-off from (C1). A comparison of different, also smooth, regulators for pure gravity computations in a flat background has been put forward in [24]. The regulator dependences of the results have been found to be small.

We close this section with a remark on the use of flat regulators in a derivative expansion. The flat regulator has been singled out by optimization theory as the the optimal one within the lowest order of the derivative expansion, see [78, 105]. To higher orders in the derivative expansion this does not hold because of the non-analyticity of the regulator. Note however, that smooth, analytic versions of the flat regulator satisfy the optimization criterion for higher order of the derivative expansion, see [78]. The latter property is potentially important for the convergence of our approximation, when we take higher order gravitationally induced terms into account, see Sec. IV. It turns out that in our projection scheme all derivatives with respect to external momentum hit the momentum-dependences of the vertices. In other words, in terms of optimization we are still in the same situation as for the lowest order of the derivative expansion, and the regulators satisfy the optimization criteria in [78, 105].

### Appendix E: Explicit form of matter-metric vertices from covariant kinetic terms

To explain the derivative structure of the quartic interactions we present the matter vertices as obtained when taking appropriate variations of the covariant kinetic terms. Note that for fermions also the variations of the spin-connection

$$\delta\Gamma_\mu = -\frac{1}{8}D_\alpha\delta g_{\beta\mu}[\gamma^\alpha, \gamma^\beta] \quad (\text{E1})$$

and the gamma-matrices

$$\delta\gamma^\mu = \frac{1}{2}\delta g^{\mu\nu}\gamma_\nu \quad (\text{E2})$$

are taken into account. For the description of spinors in gravity we use the spin-covariant derivative  $\gamma^\mu\nabla_\mu = \gamma^\mu(\partial_\mu + \Gamma_\mu)$ , where  $\Gamma^\mu$  denotes the spin connection, defined using the spin-base invariant formalism introduced in [107, 108]. Note that the results for the variations from the spin-base invariant formalism agree with those obtained in the standard vielbein formalism within a symmetric O(4) gauge [109, 110]. This allows us to rewrite vielbein fluctuations in terms of metric fluctuations.

$$\begin{aligned} & \left[ \frac{\delta}{\delta\psi(p_{\psi_1})} \frac{\delta}{\delta\bar{\psi}(p_{\psi_2})} \frac{\delta}{\delta h_{\mu\nu}(p_{h_1})} \frac{\delta}{\delta h_{\rho\sigma}(p_{h_2})} \Gamma_k \right]_{\Phi=0} \\ &= \frac{1}{8} \left[ g^{\mu\sigma} g^{\rho\nu} (\not{p}_{h_1} + \not{p}_{h_2} + \not{p}_{\psi_1}) - g^{\mu\nu} g^{\rho\sigma} (\not{p}_{h_1} + \not{p}_{h_2} + \not{p}_{\psi_1}) \right] \\ &+ \frac{1}{32} \left[ + g^{\mu\rho} g^{\nu\sigma} (5\not{p}_{h_1} + 3\not{p}_{h_2} + 8\not{p}_{\psi_1}) \right] \\ &+ \frac{1}{64} \left[ (\not{p}_{h_2} - \not{p}_{h_1}) (g^{\mu\rho} \gamma^\nu \gamma^\sigma - g^{\mu\sigma} \gamma^\nu \gamma^\rho + g^{\nu\rho} \gamma^\mu \gamma^\sigma + g^{\nu\sigma} \gamma^\mu \gamma^\rho) \right] \\ &+ \frac{1}{64} \left[ p_{h_1}^\mu (4g^{\rho\sigma} \gamma^\nu - 2g^{\nu\rho} \gamma^\sigma - 2g^{\nu\sigma} \gamma^\rho) \right. \\ &\quad + p_{h_1}^\nu (4g^{\rho\sigma} \gamma^\mu - 2g^{\mu\rho} \gamma^\sigma - 2g^{\mu\sigma} \gamma^\rho) \\ &\quad + p_{h_1}^\rho (4g^{\mu\nu} \gamma^\sigma - 4g^{\mu\sigma} \gamma^\nu - 4g^{\nu\sigma} \gamma^\mu) \\ &\quad \left. + p_{h_1}^\sigma (4g^{\mu\nu} \gamma^\rho - 4g^{\mu\rho} \gamma^\nu - 4g^{\nu\rho} \gamma^\mu) \right] \\ &+ \frac{1}{64} \left[ p_{h_2}^\mu (4g^{\rho\sigma} \gamma^\nu - 4g^{\nu\rho} \gamma^\sigma - 4g^{\nu\sigma} \gamma^\rho) \right. \\ &\quad + p_{h_2}^\nu (4g^{\rho\sigma} \gamma^\mu - 4g^{\mu\rho} \gamma^\sigma - 4g^{\mu\sigma} \gamma^\rho) \\ &\quad + p_{h_2}^\rho (4g^{\mu\nu} \gamma^\sigma - 2g^{\mu\sigma} \gamma^\nu - 2g^{\nu\sigma} \gamma^\mu) \\ &\quad \left. + p_{h_2}^\sigma (4g^{\mu\nu} \gamma^\rho - 2g^{\mu\rho} \gamma^\nu - 2g^{\nu\rho} \gamma^\mu) \right] \\ &+ \frac{1}{64} \left[ p_{\psi_1}^\mu (8g^{\rho\sigma} \gamma^\nu - 6g^{\nu\rho} \gamma^\sigma - 6g^{\nu\sigma} \gamma^\rho) \right. \\ &\quad + p_{\psi_1}^\nu (8g^{\rho\sigma} \gamma^\mu - 6g^{\mu\rho} \gamma^\sigma - 6g^{\mu\sigma} \gamma^\rho) \\ &\quad + p_{\psi_1}^\rho (8g^{\mu\nu} \gamma^\sigma - 6g^{\mu\sigma} \gamma^\nu - 6g^{\nu\sigma} \gamma^\mu) \\ &\quad \left. + p_{\psi_1}^\sigma (8g^{\mu\nu} \gamma^\rho - 6g^{\mu\rho} \gamma^\nu - 6g^{\nu\rho} \gamma^\mu) \right] \quad (\text{E3}) \end{aligned}$$

$$\begin{aligned} & \left[ \frac{\delta}{\delta\phi(p_{\phi_1})} \frac{\delta}{\delta\phi(p_{\phi_2})} \frac{\delta}{\delta h_{\mu\nu}(p_{h_1})} \Gamma_k \right]_{\Phi=0} \quad (\text{E4}) \\ &= \frac{1}{2} \left[ g^{\mu\nu} (m_\phi^2 + p_{h_1} \cdot p_{\phi_1} + p_{\phi_1} \cdot p_{\phi_1}) \right. \\ &\quad \left. + p_{\phi_1}^\mu p_{h_1}^\nu + p_{\phi_1}^\nu p_{h_1}^\mu + p_{\phi_1}^\mu p_{\phi_1}^\nu \right] \end{aligned}$$

$$\begin{aligned} & \left[ \frac{\delta}{\delta\phi(p_{\phi_1})} \frac{\delta}{\delta\phi(p_{\phi_2})} \frac{\delta}{\delta h_{\mu\nu}(p_{h_1})} \frac{\delta}{\delta h_{\rho\sigma}(p_{h_2})} \Gamma_k \right]_{\Phi=0} \quad (\text{E5}) \\ &= \frac{1}{4} \left[ -p_{\phi_1}^\sigma p_{\phi_2}^\mu g^{\rho\nu} - p_{\phi_1}^\rho p_{\phi_2}^\nu g^{\mu\sigma} - p_{\phi_1}^\sigma p_{\phi_2}^\nu g^{\mu\rho} - p_{\phi_1}^\nu p_{\phi_2}^\rho g^{\mu\sigma} \right. \\ &\quad + p_{\phi_1}^\sigma p_{\phi_2}^\rho g^{\mu\nu} - p_{\phi_1}^\mu p_{\phi_2}^\sigma g^{\rho\nu} - p_{\phi_1}^\nu p_{\phi_2}^\sigma g^{\mu\rho} + p_{\phi_1}^\rho p_{\phi_2}^\sigma g^{\mu\nu} \\ &\quad + g^{\mu\sigma} g^{\rho\nu} p_{\phi_1} \cdot p_{\phi_2} \\ &\quad + g^{\rho\sigma} (-g^{\mu\nu} p_{\phi_1} \cdot p_{\phi_2} + p_{\phi_1}^\nu p_{\phi_2}^\mu + p_{\phi_1}^\mu p_{\phi_2}^\nu) \\ &\quad \left. - g^{\nu\sigma} (-g^{\mu\rho} p_{\phi_1} \cdot p_{\phi_2} + p_{\phi_1}^\rho p_{\phi_2}^\mu + p_{\phi_1}^\mu p_{\phi_2}^\rho) \right] \end{aligned}$$

$$\begin{aligned} & \left[ \frac{\delta}{\delta\psi(p_{\psi_1})} \frac{\delta}{\delta\bar{\psi}(p_{\psi_2})} \frac{\delta}{\delta h_{\mu\nu}(p_{h_1})} \Gamma_k \right]_{\Phi=0} \quad (\text{E6}) \\ &= \frac{1}{8} \left[ -2g^{\mu\nu} (\not{p}_{h_1} + 2\not{p}_{\psi_1}) \right. \\ &\quad \left. + \gamma^\mu p_{h_1}^\nu + \gamma^\nu p_{h_1}^\mu + 2\gamma^\mu p_{\psi_1}^\nu + 2\gamma^\nu p_{\psi_1}^\mu \right] \end{aligned}$$

### Appendix F: Gauge-parameter dependence of the Yukawa $\beta$ -function

Here we present the full gauge-dependent  $\beta_y$ -function for  $\mu_\phi = 0$ . All other parameters are kept free.

$$\begin{aligned}
\beta_y = & y \left( \eta_{\psi,0} + \frac{\eta_{\phi,0}}{2} \right) + \frac{y^3 (5 - \eta_\psi)}{80\pi^2 (\mu_\phi + 1)} + \frac{y^3 (6 - \eta_\phi)}{96\pi^2 (\mu_\phi + 1)^2} \\
& yg \left[ \frac{(\eta_\psi - 6) (\beta - 2\alpha\mu_h - 3)}{5\pi (6\beta - 2\mu_h (2\alpha (\mu_h + 1) + 3) + \beta^2 (2\mu_h - 1) - 9)} \right. \\
& - \frac{12 (\eta_h - 7) ((\beta - 3)^3 - 4\alpha (2\alpha - \beta^2 + \beta) \mu_h^2 - 4\alpha (\beta - 3)^2 \mu_h)}{35\pi (-6\beta + 2\mu_h (2\alpha (\mu_h + 1) + 3) + \beta^2 (1 - 2\mu_h) + 9)^2} \\
& - \frac{\eta_h - 8}{64\pi (\alpha\mu_h + 1)^2 (-6\beta + 2\mu_h (2\alpha (\mu_h + 1) + 3) + \beta^2 (1 - 2\mu_h) + 9)^2} \times \\
& \times [(1 - \alpha)(\beta - 3)^4 + 4\alpha^3 (4\alpha - 3(\beta - 2)\beta - 7)\mu_h^4 + \mu_h^2 + 8(\alpha - 1)\alpha^2 (\beta - 3)^2 \mu_h^3 + 2\alpha(\beta - 3)^2 (-4\alpha + 3(\beta - 2)\beta + 7)\mu_h \\
& + \alpha (-16\alpha^2 + \alpha(\beta(\beta((\beta - 12)\beta + 78) - 156) + 121) - 4(\beta(\beta^3 - 3\beta - 6) + 12))] \\
& + \frac{(\eta_\psi - 7) ((\alpha - 1)(\beta - 3)^2 + \alpha(4\alpha - 3(\beta - 2)\beta - 7)\mu_h)}{56\pi (\alpha\mu_h + 1) (-6\beta + 2\mu_h (2\alpha (\mu_h + 1) + 3) + \beta^2 (1 - 2\mu_h) + 9)} \\
& - \frac{(\eta_h - 6)}{12\pi (\mu_h + 1)^2 (\alpha\mu_h + 1)^2 (-6\beta + 4\alpha\mu_h^2 + (4\alpha + 6)\mu_h + \beta^2 (1 - 2\mu_h) + 9)^2} \times \\
& \times [96\alpha^4 (\mu_h + 1)^2 \mu_h^4 - 4\alpha^3 (\mu_h + 1) \mu_h^2 (\beta^2 (2\mu_h^3 + 18\mu_h^2 - 15\mu_h - 1) + 6\beta(4\mu_h^2 + 15\mu_h + 1) - 3(6\mu_h^3 + 62\mu_h^2 + 73\mu_h + 7)) \\
& + \alpha^2 \mu_h (3\beta^4 \mu_h (6\mu_h^2 - 8\mu_h + 1) + 12\beta^3 \mu_h (\mu_h^2 + 12\mu_h - 4) + \beta^2 (-64\mu_h^4 - 412\mu_h^3 - 240\mu_h^2 + 410\mu_h + 32)) \\
& + \alpha^2 (-12\beta(31\mu_h^3 + 148\mu_h^2 + 148\mu_h + 16) + 3(64\mu_h^4 + 614\mu_h^3 + 1272\mu_h^2 + 833\mu_h + 96)) \\
& + \alpha(3\beta^4 (4\mu_h^4 + 16\mu_h^3 - 19\mu_h^2 + 1) + 12\beta^3 (8\mu_h^3 + 33\mu_h^2 - 8\mu_h - 3) - 2\beta^2 (40\mu_h^4 + 280\mu_h^3 + 177\mu_h^2 - 416\mu_h - 83)) \\
& + \alpha(-12\beta(32\mu_h^3 + 173\mu_h^2 + 200\mu_h + 29) + 3(44\mu_h^4 + 480\mu_h^3 + 1081\mu_h^2 + 768\mu_h + 93)) \\
& + 3(\beta^4 (6\mu_h^2 - 8\mu_h + 1) + 4\beta^3 (\mu_h^2 + 12\mu_h - 4) + \beta^2 (-44\mu_h^2 - 48\mu_h + 86) - 12\beta(\mu_h^2 + 12\mu_h + 16) + 3(26\mu_h^2 + 72\mu_h + 51))] \\
& + \frac{2(\eta_\phi - 6) \mu_\phi (\alpha (2\mu_h - 1) + 3)}{3\pi (\mu_\phi + 1)^2 (-6\beta + 4\alpha\mu_h^2 + (4\alpha + 6)\mu_h + \beta^2 (1 - 2\mu_h) + 9)} \\
& - \frac{12(\eta_\phi - 7) \mu_\phi (\beta - 2\alpha\mu_h - 3)}{35\pi (\mu_\phi + 1)^2 (6\beta - 2\mu_h (2\alpha (\mu_h + 1) + 3) + \beta^2 (2\mu_h - 1) - 9)} \\
& + \frac{2(\eta_h - 6) \mu_\phi ((3 - \alpha)(\beta - 3)^2 + 4\alpha(3\alpha - \beta^2) \mu_h^2 + 4\alpha(\beta - 3)^2 \mu_h)}{3\pi (\mu_\phi + 1) (6\beta - 2\mu_h (2\alpha (\mu_h + 1) + 3) + \beta^2 (2\mu_h - 1) - 9)^2} \\
& + \left. \frac{12(\eta_h - 7) \mu_\phi ((\beta - 3)^3 - 4\alpha(2\alpha - \beta^2 + \beta) \mu_h^2 - 4\alpha(\beta - 3)^2 \mu_h)}{35\pi (\mu_\phi + 1) (6\beta - 2\mu_h (2\alpha (\mu_h + 1) + 3) + \beta^2 (2\mu_h - 1) - 9)^2} \right]
\end{aligned} \tag{F1}$$

### Appendix G: Specifying Projections in the $\mathcal{X}$ sector

The quartic tensor structures the flow generated by the diagrams in Fig. 7 are restricted by the following requirements:

- All diagrams contain at least three external momenta. This is the case as the momentum of every

external scalar must appear at the vertex, accounting for two of the external momenta. The third is required, as the chiral symmetry for the fermions requires the existence of a  $\gamma$  matrix in the generated interaction. To construct a Lorentz scalar, a third momentum is then necessary to saturate the open index of the  $\gamma$  matrix.

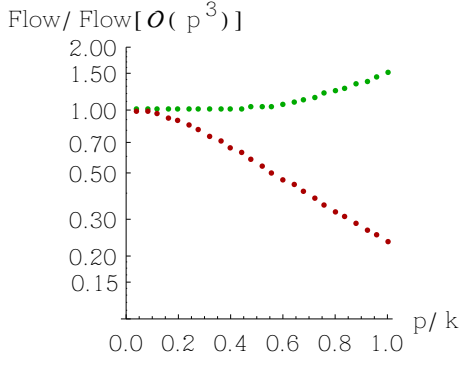


FIG. 13. Reliability of the lowest order  $\mathcal{X}_{1+2}$ - $\mathcal{X}_{3+4}$  derivative projection. The plot shows the full momentum dependence of the according projection, normalized by the numerical value of the lowest order projection. The upper green dots correspond to the  $\mathcal{X}_{1+2}$  projection, while the lower red dots indicate the values for the  $\mathcal{X}_{3+4}$  projection.

- All resulting tensor structures come with momentum-dependent scalar legs because of the structure of the  $(h)h\phi\phi$ -vertex (E5), in which no term exists with constant scalar legs.
- Further momentum structures of  $\mathcal{O}(p^5)$  and higher are generated but will not be considered in this truncation as operators with more derivatives (therefore couplings with higher canonical dimension) are expected to remain less relevant at a possible fixed point.

There are six different tensor structures satisfying the above requirements, two of which can be rewritten in terms of the other four by partial integration, when we neglect total derivatives. The induced action  $\Gamma_k$  induced contains the four quantum-gravity induced interactions of scalars and fermions which have the lowest order in a canonical power counting.

To project onto the couplings  $\mathcal{X}_1, \mathcal{X}_2, \mathcal{X}_3$  and  $\mathcal{X}_4$ , we apply functional derivatives with respect to the fields (n-point functions) and switch to momentum space ( $\partial_\mu \phi(x) \rightarrow ip_\mu \tilde{\phi}(p)$ ). For fermions we use the convention  $\partial_\mu \psi(x) \rightarrow ip_\mu \tilde{\psi}(p)$  and  $\partial_\mu \bar{\psi}(x) \rightarrow -ip_\mu \tilde{\bar{\psi}}(p)$  connected to conventions for the Fourier transformations fixed e.g. in [111]. To account for the  $\gamma$ -matrix we additionally project with an external  $\gamma_\mu p_{\text{ext}}^\mu$  such that the trace doesn't evaluate to zero. Then we make use of the identity  $\text{Tr}(\gamma_\mu p_a^\mu \gamma_\nu p_b^\nu) = 4p_a \cdot p_b$  to obtain

$$\begin{aligned} & \frac{1}{4} \text{Tr} \left( \frac{\delta}{\delta \phi(p_1)} \frac{\delta}{\delta \phi(p_2)} \frac{\delta}{\delta \psi(p_3)} \frac{\delta}{\delta \bar{\psi}(p_4)} \Gamma_k \gamma_\rho p_{\text{ext}}^\rho \right) \Big|_{\mathcal{O}(p^4)} \\ &= \mathcal{X}_1 [(p_1 \cdot p_1)(p_2 \cdot p_{\text{ext}}) + (p_2 \cdot p_2)(p_1 \cdot p_{\text{ext}})] \\ &+ \mathcal{X}_2 [(p_1 \cdot p_2)((p_1 \cdot p_{\text{ext}}) + (p_2 \cdot p_{\text{ext}}))] \\ &+ \mathcal{X}_3 [(p_2 \cdot p_3)(p_1 \cdot p_{\text{ext}}) + (p_1 \cdot p_3)(p_2 \cdot p_{\text{ext}})] \\ &+ 2\mathcal{X}_4 [(p_1 \cdot p_2)(p_3 \cdot p_{\text{ext}})] \quad . \end{aligned} \quad (\text{G1})$$

By choosing the fermion momentum to be zero ( $p_3 = 0$ ) and identifying the scalar momenta ( $p_1 = p_2 = p$ ) we project only on the first two couplings, while a momentum configuration with  $p_2 = -p_1$  singles out the latter two couplings. Thus we can project on  $\mathcal{X}_1 + \mathcal{X}_2 = \mathcal{X}_{1+2}$  as well as  $\mathcal{X}_3 + \mathcal{X}_4 = \mathcal{X}_{3+4}$  by such choices of momenta and thereafter taking derivatives with respect to the momenta, i.e.

$$\begin{aligned} & \frac{1}{8} \left[ \partial_{p^4} \text{Tr} \left( \frac{\delta}{\delta \phi(p)} \frac{\delta}{\delta \phi(p)} \frac{\delta}{\delta \psi(0)} \frac{\delta}{\delta \bar{\psi}(-2p)} \Gamma_k \gamma_\rho p^\rho \right) \right]_{p_i=0} \\ &= \mathcal{X}_1 + \mathcal{X}_2 = \mathcal{X}_{1+2} \end{aligned} \quad (\text{G2})$$

$$\begin{aligned} & \frac{1}{8} \left[ \partial_{p^4} \text{Tr} \left( \frac{\delta}{\delta \phi(p)} \frac{\delta}{\delta \phi(-p)} \frac{\delta}{\delta \psi(-p)} \frac{\delta}{\delta \bar{\psi}(p)} \Gamma_k \gamma_\rho p^\rho \right) \right]_{p_i=0} \\ &= \mathcal{X}_3 + \mathcal{X}_4 = \mathcal{X}_{3+4} \quad . \end{aligned} \quad (\text{G3})$$

When applying a derivative projection at  $p = 0$  we implicitly assume that the momentum dependence from higher orders is small or equivalently that the remaining couplings are momentum independent. To justify this assumption the approximation must be valid for momenta up to the cutoff  $k$ , i.e.  $0 < p/k < 1$ , since these are the ones which are integrated out in the loop.

We expect that the most general momentum dependence is encoded in the fully symmetric momentum configuration.

For the full system where we differentiate all four momentum structures we thus try to stick to the fully symmetric momentum configuration where all external momenta have the same absolute value and all angles between them are equal. In the given case of a four-point interaction we can eliminate the fourth momentum by momentum conservation and demand for the remaining parameters

$$p := |p_1| = |p_2| = |p_3| \quad \& \quad \vartheta_{12} = \vartheta_{13} = \vartheta_{23} = -\frac{1}{3} \quad . \quad (\text{G4})$$

For concreteness we give an explicit parametrization of such a momentum configuration

$$p_1 = \begin{pmatrix} 1 \\ 0 \\ 0 \\ 0 \end{pmatrix}, \quad p_2 = \begin{pmatrix} -1/3 \\ 2\sqrt{2}/3 \\ 0 \\ 0 \end{pmatrix}, \quad p_3 = \begin{pmatrix} -1/3 \\ -\sqrt{2}/3 \\ -\sqrt{2}/3 \\ 0 \end{pmatrix} \quad . \quad (\text{G5})$$

To be able to differentiate the four tensor structures we keep the momenta general when taking momentum derivatives and apply conditions for the external momentum (e.g.  $p_1 \cdot p_{\text{ext}} = 0$ ). In this way it is possible to project onto the four couplings in the following manner

$$\mathcal{X}_1 = \frac{3}{8\sqrt{2}} \left[ \partial_{p_1} \partial_{p_1} \partial_{p_2} \partial_{p_{\text{ext}}} \left( \text{Tr} \left[ \frac{\delta}{\delta\phi(p_1)} \frac{\delta}{\delta\phi(p_2)} \frac{\delta}{\delta\psi(p_3)} \frac{\delta}{\delta\bar{\psi}(-p_1-p_2-p_3)} \Gamma_k \gamma_\rho p_{\text{ext}}^\rho \right] \right) \right]_{p_i=0, \vartheta_{1,\text{ext}}=0, \vartheta_{2,\text{ext}}=\vartheta_{3,\text{ext}}=\sqrt{2}/3} \quad (\text{G6})$$

$$\mathcal{X}_2 = \frac{-9}{8\sqrt{2}} \left[ \partial_{p_1} \partial_{p_1} \partial_{p_2} \partial_{p_{\text{ext}}} \left( \text{Tr} \left[ \frac{\delta}{\delta\phi(p_1)} \frac{\delta}{\delta\phi(p_2)} \frac{\delta}{\delta\psi(p_3)} \frac{\delta}{\delta\bar{\psi}(-p_1-p_2-p_3)} \Gamma_k \gamma_\rho p_{\text{ext}}^\rho \right] \right) \right]_{p_i=0, \vartheta_{2,\text{ext}}=0, \vartheta_{1,\text{ext}}=\vartheta_{3,\text{ext}}=\sqrt{2}/3} \quad (\text{G7})$$

$$\mathcal{X}_3 = \frac{-9}{16\sqrt{2}} \left[ \partial_{p_1} \partial_{p_2} \partial_{p_3} \partial_{p_{\text{ext}}} \left( \text{Tr} \left[ \frac{\delta}{\delta\phi(p_1)} \frac{\delta}{\delta\phi(p_2)} \frac{\delta}{\delta\psi(p_3)} \frac{\delta}{\delta\bar{\psi}(-p_1-p_2-p_3)} \Gamma_k \gamma_\rho p_{\text{ext}}^\rho \right] \right) \right]_{p_i=0, \vartheta_{3,\text{ext}}=0, \vartheta_{1,\text{ext}}=\vartheta_{2,\text{ext}}=\sqrt{2}/3} \quad (\text{G8})$$

$$\mathcal{X}_4 = \frac{-9}{8\sqrt{2}} \left[ \partial_{p_1} \partial_{p_2} \partial_{p_3} \partial_{p_{\text{ext}}} \left( \text{Tr} \left[ \frac{\delta}{\delta\phi(p_1)} \frac{\delta}{\delta\phi(p_2)} \frac{\delta}{\delta\psi(p_3)} \frac{\delta}{\delta\bar{\psi}(-p_1-p_2-p_3)} \Gamma_k \gamma_\rho p_{\text{ext}}^\rho \right] \right) \right]_{p_i=0, \vartheta_{1,\text{ext}}=\vartheta_{2,\text{ext}}=0, \vartheta_{3,\text{ext}}=\sqrt{2}/3} \quad (\text{G9})$$

Again we state the explicit external momentum choices corresponding to the above explicit parametrization (cf. (G5)) and the projections (G6) - (G9)

$$p_{\text{ext},\mathcal{X}_1} = \begin{pmatrix} 0 \\ 1/2 \\ -\sqrt{3}/2 \\ 0 \end{pmatrix}, \quad p_{\text{ext},\mathcal{X}_2} = \begin{pmatrix} \sqrt{2}/3 \\ 1/6 \\ -\sqrt{3}/2 \\ 0 \end{pmatrix},$$

$$p_{\text{ext},\mathcal{X}_3} = \begin{pmatrix} \sqrt{2}/3 \\ 2/3 \\ -1/\sqrt{3} \\ 0 \end{pmatrix}, \quad p_{\text{ext},\mathcal{X}_4} = \begin{pmatrix} 0 \\ 0 \\ -1 \\ 0 \end{pmatrix}. \quad (\text{G10})$$

#### Appendix H: Analytic $\beta$ -functions in the $\mathcal{X}$ -sector

Here we present the full  $\beta$ -functions in the  $\mathcal{X}$ -sector. Firstly those for the simplified system with projections on  $\mathcal{X}_{1+2}$  (cf. (G2)) and  $\mathcal{X}_{1+2}$  (cf. (G3)) and then those for the fully disentangled system, cf. (G6)-(G9).

$$\beta_{\mathcal{X}_{1+2}} = \mathcal{X}_{1+2} (4 + \eta_{\phi,0} + \eta_{\psi,0}) - \frac{g(\eta_\psi - 8)(7\mathcal{X}_{1+2} - 9\mathcal{X}_{3+4})}{448\pi(\mu_h + 1)} - \frac{g(\eta_\psi - 7)(4\mathcal{X}_{1+2} + 5\mathcal{X}_{3+4})}{112\pi(\mu_h + 1)} - \frac{g(\eta_\psi - 6)(8\mathcal{X}_{1+2} - 19\mathcal{X}_{3+4})}{480\pi(\mu_h + 1)} \quad (\text{H1})$$

$$- \frac{g(\eta_\phi - 9)(7\mathcal{X}_{1+2} - 9\mathcal{X}_{3+4})}{252\pi(\mu_h + 1)} - \frac{g(\eta_\phi - 8)(10\mathcal{X}_{1+2} - 3\mathcal{X}_{3+4})}{192\pi(\mu_h + 1)} - \frac{g(\eta_h - 9)(7\mathcal{X}_{1+2} - 9\mathcal{X}_{3+4})}{252\pi(\mu_h + 1)^2}$$

$$- \frac{g(\eta_h - 8)(10\mathcal{X}_{1+2} - 3\mathcal{X}_{3+4})}{192\pi(\mu_h + 1)^2} - \frac{g(\eta_h - 8)(4\mathcal{X}_{1+2} + 11\mathcal{X}_{3+4})}{128\pi(\mu_h + 1)^2} - \frac{g(\eta_h - 7)(8\mathcal{X}_{1+2} - 17\mathcal{X}_{3+4})}{140\pi(\mu_h + 1)^2}$$

$$- \frac{11\mathcal{X}_{1+2}(\eta_\psi - 8)(\mathcal{X}_{1+2} - \mathcal{X}_{3+4})}{896\pi^2} + \frac{\mathcal{X}_{1+2}(\eta_\phi - 9)(5\mathcal{X}_{1+2} - 47\mathcal{X}_{3+4})}{2016\pi^2} - \frac{g\mathcal{X}_{1+2}(\eta_\psi - 8)}{64\pi(\mu_h + 1)} + \frac{g\mathcal{X}_{1+2}(\eta_\psi - 6)}{40\pi(\mu_h + 1)}$$

$$- \frac{g\mathcal{X}_{1+2}(\eta_\phi - 9)}{36\pi(\mu_h + 1)} - \frac{g\mathcal{X}_{1+2}(\eta_h - 9)}{36\pi(\mu_h + 1)^2} + \frac{7g\mathcal{X}_{1+2}(\eta_h - 6)}{16\pi(\mu_h + 1)^2} - \frac{g^2(\eta_\psi - 6)}{6(\mu_h + 1)^2} - \frac{3g^2(\eta_h - 7)}{7(\mu_h + 1)^3} - \frac{5g^2(\eta_h - 6)}{3(\mu_h + 1)^3}$$

$$\beta_{\mathcal{X}_{3+4}} = \mathcal{X}_{3+4} (\eta_{\psi,0} + \eta_{\phi,0} + 4) + \frac{g(\eta_\psi - 6)(140\mathcal{X}_{1+2} - 93\mathcal{X}_{3+4})}{960\pi(\mu_h + 1)} - \frac{(\eta_\psi - 8)(-44\mathcal{X}_{1+2}\mathcal{X}_{3+4} + 22\mathcal{X}_{1+2}^2 + 19\mathcal{X}_{3+4}^2)}{1792\pi^2} \quad (\text{H2})$$

$$+ \frac{(\eta_\phi - 9)(-3\mathcal{X}_{1+2}\mathcal{X}_{3+4} + 5\mathcal{X}_{1+2}^2 - 38\mathcal{X}_{3+4}^2)}{2016\pi^2} - \frac{9g\mathcal{X}_{3+4}(\eta_\psi - 7)}{112\pi(\mu_h + 1)} - \frac{15g\mathcal{X}_{3+4}(\eta_h - 8)}{128\pi(\mu_h + 1)^2} - \frac{g\mathcal{X}_{3+4}(\eta_h - 7)}{140\pi(\mu_h + 1)^2}$$

$$+ \frac{7g\mathcal{X}_{3+4}(\eta_h - 6)}{16\pi(\mu_h + 1)^2} - \frac{g^2(\eta_\psi - 6)}{6(\mu_h + 1)^2} - \frac{3g^2(\eta_h - 7)}{7(\mu_h + 1)^3} - \frac{5g^2(\eta_h - 6)}{3(\mu_h + 1)^3}$$

$$\begin{aligned}
\beta_{\mathcal{X}_1} = & \mathcal{X}_1 (\eta_{\psi,0} + \eta_{\phi,0} + 4) - \frac{g^2 (\eta_{\psi} - 6)}{9 (\mu_h + 1)^2} - \frac{2g^2 (\eta_h - 7)}{7 (\mu_h + 1)^3} - \frac{10g^2 (\eta_h - 6)}{9 (\mu_h + 1)^3} - \frac{g (36\mathcal{X}_1 + 10\mathcal{X}_2 - 23\mathcal{X}_3 - 10\mathcal{X}_4) (\eta_{\psi} - 8)}{1344\pi (\mu_h + 1)} \quad (\text{H3}) \\
& - \frac{g (6\mathcal{X}_1 - 5\mathcal{X}_3) (\eta_{\psi} - 7)}{336\pi (\mu_h + 1)} + \frac{g\mathcal{X}_1 (\eta_{\psi} - 6)}{80\pi (\mu_h + 1)} + \frac{g (9\mathcal{X}_1 - 8\mathcal{X}_2 + 4\mathcal{X}_3) (\eta_{\psi} - 6)}{720\pi (\mu_h + 1)} - \frac{g (36\mathcal{X}_1 + 10\mathcal{X}_2 - 23\mathcal{X}_3 - 10\mathcal{X}_4) (\eta_{\phi} - 9)}{756\pi (\mu_h + 1)} \\
& - \frac{g (12\mathcal{X}_1 - 10\mathcal{X}_2 - \mathcal{X}_3 + 10\mathcal{X}_4) (\eta_{\phi} - 8)}{576\pi (\mu_h + 1)} - \frac{g (36\mathcal{X}_1 + 10\mathcal{X}_2 - 23\mathcal{X}_3 - 10\mathcal{X}_4) (\eta_h - 9)}{756\pi (\mu_h + 1)^2} - \frac{g (12\mathcal{X}_1 - \mathcal{X}_3) (\eta_h - 8)}{768\pi (\mu_h + 1)^2} \\
& - \frac{g (12\mathcal{X}_1 - 10\mathcal{X}_2 - \mathcal{X}_3 + 10\mathcal{X}_4) (\eta_h - 8)}{576\pi (\mu_h + 1)^2} + \frac{3g\mathcal{X}_1 (\eta_h - 7)}{140\pi (\mu_h + 1)^2} + \frac{g (36\mathcal{X}_1 - 52\mathcal{X}_2 + \mathcal{X}_3) (\eta_h - 7)}{1680\pi (\mu_h + 1)^2} \\
& + \frac{g (13\mathcal{X}_1 + 4\mathcal{X}_2) (\eta_h - 6)}{96\pi (\mu_h + 1)^2} - \frac{\mathcal{X}_1 (2\mathcal{X}_1 + \mathcal{X}_2) (\eta_{\psi} - 8)}{896\pi^2} - \frac{(\mathcal{X}_1 (4\mathcal{X}_2 + 3\mathcal{X}_3 + 2\mathcal{X}_4) + \mathcal{X}_2 (\mathcal{X}_2 - 2 (3\mathcal{X}_3 + \mathcal{X}_4))) (\eta_{\psi} - 8)}{1792\pi^2} \\
& - \frac{\mathcal{X}_1 (2\mathcal{X}_1 + \mathcal{X}_2) (\eta_{\phi} - 9)}{504\pi^2} + \frac{(42\mathcal{X}_1^2 + 6 (3\mathcal{X}_2 - 2 (5\mathcal{X}_3 + \mathcal{X}_4)) \mathcal{X}_1 + \mathcal{X}_2 (\mathcal{X}_2 - 13\mathcal{X}_3 - 2\mathcal{X}_4)) (\eta_{\phi} - 9)}{6048\pi^2}
\end{aligned}$$

$$\begin{aligned}
\beta_{\mathcal{X}_2} = & \mathcal{X}_2 (\eta_{\psi,0} + \eta_{\phi,0} + 4) - \frac{g^2 (\eta_{\psi} - 6)}{18 (\mu_h + 1)^2} - \frac{g^2 (\eta_h - 7)}{7 (\mu_h + 1)^3} - \frac{5g^2 (\eta_h - 6)}{9 (\mu_h + 1)^3} + \frac{g (2\mathcal{X}_2 - \mathcal{X}_3 - 2\mathcal{X}_4) (\eta_{\psi} - 8)}{672\pi (\mu_h + 1)} - \frac{\mathcal{X}_2^2 (\eta_{\phi} - 9)}{1008\pi^2} \quad (\text{H4}) \\
& - \frac{g (3\mathcal{X}_2 + \mathcal{X}_3 + 9\mathcal{X}_4) (\eta_{\psi} - 7)}{168\pi (\mu_h + 1)} + \frac{g\mathcal{X}_2 (\eta_{\psi} - 6)}{80\pi (\mu_h + 1)} - \frac{g (26\mathcal{X}_2 - 13\mathcal{X}_3 - 36\mathcal{X}_4) (\eta_{\psi} - 6)}{1440\pi (\mu_h + 1)} + \frac{g (2\mathcal{X}_2 - \mathcal{X}_3 - 2\mathcal{X}_4) (\eta_{\phi} - 9)}{378\pi (\mu_h + 1)} \\
& + \frac{g (-12\mathcal{X}_1 - 2\mathcal{X}_2 + 7\mathcal{X}_3 + 2\mathcal{X}_4) (\eta_{\phi} - 8)}{288\pi (\mu_h + 1)} + \frac{g (2\mathcal{X}_2 - \mathcal{X}_3 - 2\mathcal{X}_4) (\eta_h - 9)}{378\pi (\mu_h + 1)^2} + \frac{g (-12\mathcal{X}_1 - 2\mathcal{X}_2 + 7\mathcal{X}_3 + 2\mathcal{X}_4) (\eta_h - 8)}{288\pi (\mu_h + 1)^2} \\
& - \frac{g (12\mathcal{X}_2 + 13\mathcal{X}_3 + 54\mathcal{X}_4) (\eta_h - 8)}{768\pi (\mu_h + 1)^2} + \frac{3g\mathcal{X}_2 (\eta_h - 7)}{140\pi (\mu_h + 1)^2} - \frac{g (152\mathcal{X}_2 - 41\mathcal{X}_3 - 162\mathcal{X}_4) (\eta_h - 7)}{1680\pi (\mu_h + 1)^2} + \frac{g (8\mathcal{X}_1 + 17\mathcal{X}_2) (\eta_h - 6)}{96\pi (\mu_h + 1)^2} \\
& - \frac{(4\mathcal{X}_1 (2\mathcal{X}_2 - \mathcal{X}_3 - 3\mathcal{X}_4) + \mathcal{X}_2 (3\mathcal{X}_2 - \mathcal{X}_3 - 2\mathcal{X}_4)) (\eta_{\psi} - 8)}{1792\pi^2} - \frac{(3\mathcal{X}_1 (\mathcal{X}_2 + 3\mathcal{X}_3 + 2\mathcal{X}_4) + \mathcal{X}_2 (-\mathcal{X}_2 + 4\mathcal{X}_3 + 8\mathcal{X}_4)) (\eta_{\phi} - 9)}{3024\pi^2}
\end{aligned}$$

$$\begin{aligned}
\beta_{\mathcal{X}_3} = & \mathcal{X}_3 (\eta_{\psi,0} + \eta_{\phi,0} + 4) - \frac{g^2 (\eta_{\psi} - 6)}{9 (\mu_h + 1)^2} - \frac{2g^2 (\eta_h - 7)}{7 (\mu_h + 1)^3} - \frac{10g^2 (\eta_h - 6)}{9 (\mu_h + 1)^3} + \frac{g\mathcal{X}_3 (\eta_{\psi} - 7)}{168\pi (\mu_h + 1)} + \frac{g (9\mathcal{X}_3 - 8\mathcal{X}_4) (\eta_{\psi} - 6)}{720\pi (\mu_h + 1)} \quad (\text{H5}) \\
& - \frac{5g\mathcal{X}_3 (\eta_h - 8)}{768\pi (\mu_h + 1)^2} + \frac{g (11\mathcal{X}_3 - 52\mathcal{X}_4) (\eta_h - 7)}{1680\pi (\mu_h + 1)^2} + \frac{g (17\mathcal{X}_3 + 8\mathcal{X}_4) (\eta_h - 6)}{192\pi (\mu_h + 1)^2} \\
& - \frac{(4\mathcal{X}_1^2 + (6\mathcal{X}_2 - 7\mathcal{X}_3 - 6\mathcal{X}_4) \mathcal{X}_1 + (\mathcal{X}_2 - 2\mathcal{X}_3)^2 + 2 (\mathcal{X}_3 - \mathcal{X}_2) \mathcal{X}_4) (\eta_{\psi} - 8)}{1792\pi^2} \\
& + \frac{(18\mathcal{X}_1^2 + 3 (2\mathcal{X}_2 - 7\mathcal{X}_3 - 2\mathcal{X}_4) \mathcal{X}_1 + \mathcal{X}_2^2 - 2\mathcal{X}_2 (2\mathcal{X}_3 + \mathcal{X}_4) - 12\mathcal{X}_3 (2\mathcal{X}_3 + \mathcal{X}_4)) (\eta_{\phi} - 9)}{6048\pi^2}
\end{aligned}$$

$$\begin{aligned}
\beta_{\mathcal{X}_4} = & \mathcal{X}_4 (\eta_{\psi,0} + \eta_{\phi,0} + 4) + \frac{\sqrt{3}g^2 (\eta_h - 7)}{7 (\mu_h + 1)^3} + \frac{5g^2 (\eta_h - 6)}{3\sqrt{3} (\mu_h + 1)^3} - \frac{g (7\mathcal{X}_3 + 24\mathcal{X}_4) (\eta_{\psi} - 7)}{112\sqrt{3}\pi (\mu_h + 1)} - \frac{g (9\mathcal{X}_3 - 44\mathcal{X}_4) (\eta_{\psi} - 6)}{480\sqrt{3}\pi (\mu_h + 1)} \quad (\text{H6}) \\
& + \frac{g (16\pi g (\eta_{\psi} - 6) + 12\mathcal{X}_3 (\eta_h - 6) + 39\mathcal{X}_4 (\eta_h - 6))}{96\sqrt{3}\pi (\mu_h + 1)^2} - \frac{g (7\mathcal{X}_3 + 33\mathcal{X}_4) (\eta_h - 8)}{128\sqrt{3}\pi (\mu_h + 1)^2} - \frac{g (2\mathcal{X}_3 - 7\mathcal{X}_4) (\eta_h - 7)}{40\sqrt{3}\pi (\mu_h + 1)^2} \\
& + \frac{\sqrt{3} (4\mathcal{X}_1^2 - 2\mathcal{X}_2 \mathcal{X}_1 - 3\mathcal{X}_3 \mathcal{X}_1 - 2\mathcal{X}_2^2 + \mathcal{X}_3^2 - 4\mathcal{X}_4^2 + 3\mathcal{X}_2 \mathcal{X}_3 + 2 (\mathcal{X}_1 + 2\mathcal{X}_2 - 2\mathcal{X}_3) \mathcal{X}_4) (\eta_{\psi} - 8)}{1792\pi^2} \\
& + \frac{(-18\mathcal{X}_1^2 + 12 (-\mathcal{X}_2 + 2\mathcal{X}_3 + \mathcal{X}_4) \mathcal{X}_1 - 5\mathcal{X}_2^2 + \mathcal{X}_2 (11\mathcal{X}_3 + 10\mathcal{X}_4) + 6 (\mathcal{X}_3^2 - 4\mathcal{X}_4 \mathcal{X}_3 - 4\mathcal{X}_4^2)) (\eta_{\phi} - 9)}{2016\sqrt{3}\pi^2}
\end{aligned}$$

### Appendix I: Fixed points of the fully interacting matter system

The numerical fixed point solutions of the fully disentangled  $\mathcal{X}_i$ -truncation are given for selected values of the

gravitational couplings, cf. Tab. II. Where  $g$  is explic-

$g$	$\mathcal{X}_1^*$	$\mathcal{X}_2^*$	$\mathcal{X}_3^*$	$\mathcal{X}_4^*$	$\theta_1$	$\theta_2$	$\theta_3$	$\theta_4$	
0	0	0	0	0	-4	-4	-4	-4	GFP
0	0	0	-1417	1361	6.92	4	-4.85	-12.6	NGFP1
0	-94.87	-1138.	-656.7	-659.8	7.17	5.92	4.00	2.94	NGFP2
0	-3.050	-1907	-1091	383.7	9.39	4.00	3.47	-10.8	NGFP3
0	0	0	0	-425.5	4.00	-2.42	-2.85	-3.78	NGFP4
0	0	0	-622.9	-228.0	5.52	4.00	3.12	-3.21	NGFP5
0	-	-	-	-	-	-	-	-	NUCFP1
0	-	-	-	-	-	-	-	-	NUCFP2
1	-2.431	-1.270	-2.472	2.150	-3.76	-3.91 -0.02 i	-3.91 +0.02 i	-4.11	sGFP
1	58.51	25.46	-1385.	1345.	6.29	4.09	-5.09	-12.0	NGFP1
1	-68.90	-1126.	-626.0	-646.4	6.92	5.51	3.61	3.05	NGFP2
1	27.86	-1908.	-1061.	367.5	8.81	4.41	3.23	-10.6	NGFP3
1	-4.561	5.527	-1.077	-412.7	3.91	-2.70 - 0.13 i	-2.70 + 0.13 i	-3.56	NGFP4
1	58.58	-25.41	-589.8	-217.0	5.72	2.99 - 0.67 i	2.99 + 0.67 i	-3.21	NGFP5
1	-	-	-	-	-	-	-	-	NUCFP1
1	-	-	-	-	-	-	-	-	NUCFP2
6	-232.5	-201.7	-204.1	108.0	-0.152	-2.53	-3.13	-5.49	sGFP
6	499.2	188.9	-1234.	1258.	3.95 - 1.97 i	3.95 + 1.97 i	-7.26 - 2.89 i	-7.26 + 2.89 i	NGFP1
6	153.7	-1189.	-428.8	-599.7	5.68	3.25	2.30 - 1.68 i	2.30 + 1.68 i	NGFP2
6	229.5	-1998.	-912.3	277.4	6.03 - 2.61 i	6.03 + 2.61 i	2.72	-9.48	NGFP3
6	-208.7	92.77	-117.1	-396.7	5.06	-1.72 - 1.82 i	-1.72 + 1.82 i	-2.25	NGFP4
6	637.8	-57.51	-602.2	58.90	6.41	0.76 - 3.49 i	0.76 + 3.49 i	-3.55	NGFP5
6	-516.4	-619.7	-204.3	-362.9	2.04 - 1.54 i	2.04 + 1.54 i	-2.17 - 1.43 i	-2.17 + 1.43 i	NUCFP1
6	-259.7	-234.1	-219.7	103.1	0.153	-2.37	-2.98	-5.58	NUCFP2
6.5	-	-	-	-	-	-	-	-	sGFP
6.5	559.5	204.6	-1220.	1245.	3.86 - 2.08 i	3.86 + 2.08 i	-7.08 - 3.28 i	-7.08 + 3.28 i	NGFP1
6.5	188.6	-1212.	-409.4	-599.6	5.61	3.09	2.20 - 1.87 i	2.20 + 1.87 i	NGFP2
6.5	254.4	-2018.	-900.7	271.3	5.99 - 2.85 i	5.99 + 2.85 i	2.73	-9.43	NGFP3
6.5	-259.2	129.5	-136.8	-398.6	5.38	-1.53 - 2.16 i	-1.53 + 2.16 i	-2.20	NGFP4
6.5	701.2	-47.90	-623.0	103.2	6.50	0.60 - 3.75 i	0.60 + 3.75 i	-3.52	NGFP5
6.5	-558.4	-602.2	-201.0	-408.2	2.41 - 1.87 i	2.41 + 1.87 i	-1.96 - 1.78 i	-1.96 + 1.78 i	NUCFP1
6.5	-	-	-	-	-	-	-	-	NUCFP2
$g^*, \mu_h^*, \mu_\phi^*, \eta_{\Phi_i}^*$	-8.635	-4.701	-8.547	7.783	-4.639	-4.312	-4.231	-4.086	sGFP
$g^*, \mu_h^*, \mu_\phi^*, \eta_{\Phi_i}^*$	118.7	66.65	-1589.	1579.	-13.34	6.926	-6.198	4.877	NGFP1
$g^*, \mu_h^*, \mu_\phi^*, \eta_{\Phi_i}^*$	43.69	-1270.	-691.1	-703.8	7.63	5.82	3.66 - 0.08 i	3.66 + 0.08 i	NGFP2
$g^*, \mu_h^*, \mu_\phi^*, \eta_{\Phi_i}^*$	69.98	-2224.	-1207.	422.0	-11.9	9.84	5.48	3.65	NGFP3
$g^*, \mu_h^*, \mu_\phi^*, \eta_{\Phi_i}^*$	-11.39	-1.846	-9.031	-441.7	4.22	-3.46	-3.24 - 0.29 i	-3.24 + 0.29 i	NGFP4
$g^*, \mu_h^*, \mu_\phi^*, \eta_{\Phi_i}^*$	118.2	-56.07	-653.7	-230.6	6.65	-3.54	3.08 - 1.15 i	3.08 + 1.15 i	NGFP5
$g^*, \mu_h^*, \mu_\phi^*, \eta_{\Phi_i}^*$	-	-	-	-	-	-	-	-	NUCFP1
$g^*, \mu_h^*, \mu_\phi^*, \eta_{\Phi_i}^*$	-	-	-	-	-	-	-	-	NUCFP2

TABLE II. Fixed-point values and critical exponents in the fully disentangled  $\mathcal{X}_i$ -truncation (all other matter couplings set to zero) for  $g = 0$ ,  $g = 1$ ,  $g = 6$  and  $g = 6.5$  for vanishing metric mass parameter and vanishing anomalous dimensions. We give values for all 8 fixed points that become real for some values of  $g$ . Where the fixed point coordinates have complex-valued contributions we do not state them. In the last block the values  $g^*$ ,  $\mu_h^*$ ,  $\mu_\phi^*$  and  $\eta_{\Phi_i}^*$  refer to the fixed point values from [57].

itly stated  $\mu_h = \eta_h = \eta_\psi = \eta_\phi = 0$  holds. The last value corresponds to the non-interacting matter-gravity fixed

point found in [57], i.e.  $g^* = 0.5503$ ,  $\mu_h^* = -0.5848$  and  $\lambda_3^* = 0.1001$ .

- 
- [1] S. Weinberg, General Relativity: An Einstein centenary survey, Eds. Hawking, S.W., Israel, W; Cambridge University Press, 790 (1979).
- [2] M. Reuter, Phys. Rev. **D57**, 971 (1998), arXiv:hep-th/9605030.
- [3] D. Dou and R. Percacci, Class. Quant. Grav. **15**, 3449 (1998), arXiv:hep-th/9707239 [hep-th].
- [4] W. Souma, Prog.Theor.Phys. **102**, 181 (1999), arXiv:hep-th/9907027 [hep-th].
- [5] M. Reuter and F. Saueressig, Phys. Rev. **D65**, 065016 (2002), arXiv:hep-th/0110054 [hep-th].
- [6] O. Lauscher and M. Reuter, Phys. Rev. **D65**, 025013 (2002), arXiv:hep-th/0108040.
- [7] O. Lauscher and M. Reuter, Phys. Rev. **D66**, 025026 (2002), arXiv:hep-th/0205062.
- [8] D. F. Litim, Phys.Rev.Lett. **92**, 201301 (2004), arXiv:hep-th/0312114 [hep-th].

- [9] J. M. Pawłowski, (2003), arXiv:hep-th/0310018 [hep-th].
- [10] P. Fischer and D. F. Litim, Phys.Lett. **B638**, 497 (2006), arXiv:hep-th/0602203 [hep-th].
- [11] P. F. Machado and F. Saueressig, Phys. Rev. **D77**, 124045 (2008), arXiv:0712.0445 [hep-th].
- [12] A. Eichhorn, H. Gies, and M. M. Scherer, Phys. Rev. **D80**, 104003 (2009), arXiv:0907.1828 [hep-th].
- [13] A. Codello and R. Percacci, Phys. Rev. Lett. **97**, 221301 (2006), arXiv:hep-th/0607128.
- [14] A. Codello, R. Percacci, and C. Rahmede, Annals Phys. **324**, 414 (2009), arXiv:0805.2909 [hep-th].
- [15] D. Benedetti, P. F. Machado, and F. Saueressig, Mod. Phys. Lett. **A24**, 2233 (2009), arXiv:0901.2984 [hep-th].
- [16] E. Manrique and M. Reuter, Annals Phys. **325**, 785 (2010), arXiv:0907.2617 [gr-qc].
- [17] A. Eichhorn and H. Gies, Phys. Rev. **D81**, 104010 (2010), arXiv:1001.5033 [hep-th].
- [18] K. Groh and F. Saueressig, J. Phys. **A43**, 365403 (2010), arXiv:1001.5032 [hep-th].
- [19] E. Manrique, M. Reuter, and F. Saueressig, Annals Phys. **326**, 440 (2011), arXiv:1003.5129 [hep-th].
- [20] E. Manrique, M. Reuter, and F. Saueressig, Annals Phys. **326**, 463 (2011), arXiv:1006.0099 [hep-th].
- [21] J. E. Daum and M. Reuter, Phys. Lett. **B710**, 215 (2012), arXiv:1012.4280 [hep-th].
- [22] E. Manrique, S. Rechenberger, and F. Saueressig, Phys.Rev.Lett. **106**, 251302 (2011), arXiv:1102.5012 [hep-th].
- [23] I. Donkin and J. M. Pawłowski, (2012), arXiv:1203.4207 [hep-th].
- [24] N. Christiansen, D. F. Litim, J. M. Pawłowski, and A. Rodigast, Phys.Lett. **B728**, 114 (2014), arXiv:1209.4038 [hep-th].
- [25] S. Rechenberger and F. Saueressig, JHEP **03**, 010 (2013), arXiv:1212.5114 [hep-th].
- [26] D. Benedetti and F. Caravelli, JHEP **06**, 017 (2012), [Erratum: JHEP10,157(2012)], arXiv:1204.3541 [hep-th].
- [27] J. A. Dietz and T. R. Morris, JHEP **01**, 108 (2013), arXiv:1211.0955 [hep-th].
- [28] A. Codello, G. D'Odorico, and C. Pagani, Phys. Rev. **D89**, 081701 (2014), arXiv:1304.4777 [gr-qc].
- [29] K. Falls, D. Litim, K. Nikolakopoulos, and C. Rahmede, (2013), arXiv:1301.4191 [hep-th].
- [30] D. Benedetti, Europhys. Lett. **102**, 20007 (2013), arXiv:1301.4422 [hep-th].
- [31] J. E. Daum and M. Reuter, Annals Phys. **334**, 351 (2013), arXiv:1301.5135 [hep-th].
- [32] N. Ohta and R. Percacci, Class. Quant. Grav. **31**, 015024 (2014), arXiv:1308.3398 [hep-th].
- [33] M. Demmel, F. Saueressig, and O. Zanusso, JHEP **06**, 026 (2014), arXiv:1401.5495 [hep-th].
- [34] K. Falls, D. F. Litim, K. Nikolakopoulos, and C. Rahmede, (2014), arXiv:1410.4815 [hep-th].
- [35] D. Becker and M. Reuter, Annals Phys. **350**, 225 (2014), arXiv:1404.4537 [hep-th].
- [36] N. Christiansen, B. Knorr, J. M. Pawłowski, and A. Rodigast, Phys. Rev. **D93**, 044036 (2016), arXiv:1403.1232 [hep-th].
- [37] K. Falls, Phys. Rev. **D92**, 124057 (2015), arXiv:1501.05331 [hep-th].
- [38] K. Falls, (2015), arXiv:1503.06233 [hep-th].
- [39] J. A. Dietz and T. R. Morris, JHEP **04**, 118 (2015), arXiv:1502.07396 [hep-th].
- [40] H. Gies, B. Knorr, and S. Lippoldt, Phys. Rev. **D92**, 084020 (2015), arXiv:1507.08859 [hep-th].
- [41] M. Demmel, F. Saueressig, and O. Zanusso, JHEP **08**, 113 (2015), arXiv:1504.07656 [hep-th].
- [42] N. Christiansen, B. Knorr, J. Meibohm, J. M. Pawłowski, and M. Reichert, Phys. Rev. **D92**, 121501 (2015), arXiv:1506.07016 [hep-th].
- [43] H. Gies, B. Knorr, S. Lippoldt, and F. Saueressig, (2016), arXiv:1601.01800 [hep-th].
- [44] P. Labus, T. R. Morris, and Z. H. Slade, (2016), arXiv:1603.04772 [hep-th].
- [45] M. Niedermaier and M. Reuter, Living Rev. Rel. **9**, 5 (2006).
- [46] M. Niedermaier, Class. Quant. Grav. **24**, R171 (2007), arXiv:gr-qc/0610018 [gr-qc].
- [47] R. Percacci, (2007), arXiv:0709.3851 [hep-th].
- [48] D. F. Litim, (2008), [PoSQG-Ph,024(2007)], arXiv:0810.3675 [hep-th].
- [49] D. F. Litim, Phil. Trans. Roy. Soc. Lond. **A369**, 2759 (2011), arXiv:1102.4624 [hep-th].
- [50] M. Reuter and F. Saueressig, New J. Phys. **14**, 055022 (2012), arXiv:1202.2274 [hep-th].
- [51] M. Reuter and F. Saueressig, Lect. Notes Phys. **863**, 185 (2013), arXiv:1205.5431 [hep-th].
- [52] H. Gies and M. M. Scherer, Eur. Phys. J. **C66**, 387 (2010), arXiv:0901.2459 [hep-th].
- [53] J. Braun, H. Gies, and D. D. Scherer, Phys. Rev. **D83**, 085012 (2011), arXiv:1011.1456 [hep-th].
- [54] D. F. Litim and F. Sannino, JHEP **12**, 178 (2014), arXiv:1406.2337 [hep-th].
- [55] P. Donà, A. Eichhorn, and R. Percacci, Phys.Rev. **D89**, 084035 (2014), arXiv:1311.2898 [hep-th].
- [56] P. Donà, A. Eichhorn, and R. Percacci, Can. J. Phys. **93**, 988 (2015), arXiv:1410.4411 [gr-qc].
- [57] J. Meibohm, J. M. Pawłowski, and M. Reichert, (2015), arXiv:1510.07018 [hep-th].
- [58] P. Donà, A. Eichhorn, P. Labus, and R. Percacci, (2015), arXiv:1512.01589 [gr-qc].
- [59] O. Zanusso, L. Zambelli, G. P. Vacca, and R. Percacci, Phys. Lett. **B689**, 90 (2010), arXiv:0904.0938 [hep-th].
- [60] G. Narain and R. Percacci, Class. Quant. Grav. **27**, 075001 (2010), arXiv:0911.0386 [hep-th].
- [61] J.-E. Daum, U. Harst, and M. Reuter, JHEP **1001**, 084 (2010), arXiv:0910.4938 [hep-th].
- [62] G. P. Vacca and O. Zanusso, Phys. Rev. Lett. **105**, 231601 (2010), arXiv:1009.1735 [hep-th].
- [63] J. E. Daum, U. Harst, and M. Reuter, (2010), arXiv:1005.1488 [hep-th].
- [64] U. Harst and M. Reuter, JHEP **05**, 119 (2011), arXiv:1101.6007 [hep-th].
- [65] S. Folkerts, D. F. Litim, and J. M. Pawłowski, Phys.Lett. **B709**, 234 (2012), arXiv:1101.5552 [hep-th].
- [66] A. Eichhorn and H. Gies, New J. Phys. **13**, 125012 (2011), arXiv:1104.5366 [hep-th].
- [67] A. Eichhorn, Phys. Rev. **D86**, 105021 (2012), arXiv:1204.0965 [gr-qc].
- [68] K.-y. Oda and M. Yamada, (2015), arXiv:1510.03734 [hep-th].
- [69] J. Meibohm and J. M. Pawłowski, (2016), arXiv:1601.04597 [hep-th].
- [70] M. Shaposhnikov and C. Wetterich, Phys. Lett. **B683**, 196 (2010), arXiv:0912.0208 [hep-th].

- [71] F. Bezrukov, M. Yu. Kalmykov, B. A. Kniehl, and M. Shaposhnikov, *JHEP* **10**, 140 (2012), arXiv:1205.2893 [hep-ph].
- [72] D. Buttazzo, G. Degrassi, P. P. Giardino, G. F. Giudice, F. Sala, A. Salvio, and A. Strumia, *JHEP* **12**, 089 (2013), arXiv:1307.3536 [hep-ph].
- [73] R. Kallosh, A. D. Linde, D. A. Linde, and L. Susskind, *Phys. Rev.* **D52**, 912 (1995), arXiv:hep-th/9502069 [hep-th].
- [74] J. Berges, N. Tetradis, and C. Wetterich, *Phys. Rept.* **363**, 223 (2002), arXiv:hep-ph/0005122 [hep-ph].
- [75] K. Aoki, *Int. J. Mod. Phys.* **B14**, 1249 (2000).
- [76] C. Bagnuls and C. Bervillier, *Phys. Rept.* **348**, 91 (2001), arXiv:hep-th/0002034 [hep-th].
- [77] J. Polonyi, *Central Eur. J. Phys.* **1**, 1 (2003), arXiv:hep-th/0110026 [hep-th].
- [78] J. M. Pawłowski, *Annals Phys.* **322**, 2831 (2007), arXiv:hep-th/0512261 [hep-th].
- [79] H. Gies, *Lect. Notes Phys.* **852**, 287 (2012), arXiv:hep-ph/0611146 [hep-ph].
- [80] B. Delamotte, *Lect. Notes Phys.* **852**, 49 (2012), arXiv:cond-mat/0702365 [cond-mat.stat-mech].
- [81] J. Braun, *J. Phys.* **G39**, 033001 (2012), arXiv:1108.4449 [hep-ph].
- [82] O. J. Rosten, *Phys. Rept.* **511**, 177 (2012), arXiv:1003.1366 [hep-th].
- [83] C. Wetterich, *Phys.Lett.* **B301**, 90 (1993).
- [84] U. Ellwanger, *Z. Phys.* **C62**, 503 (1994), [,206(1993)], arXiv:hep-ph/9308260 [hep-ph].
- [85] T. R. Morris, *Int. J. Mod. Phys.* **A9**, 2411 (1994), arXiv:hep-ph/9308265.
- [86] D. F. Litim and J. M. Pawłowski (1998) pp. 168–185, arXiv:hep-th/9901063 [hep-th].
- [87] S. P. Robinson and F. Wilczek, *Phys. Rev. Lett.* **96**, 231601 (2006), arXiv:hep-th/0509050.
- [88] A. R. Pietrykowski, *Phys. Rev. Lett.* **98**, 061801 (2007), arXiv:hep-th/0606208.
- [89] D. Ebert, J. Plefka, and A. Rodigast, *Phys. Lett.* **B660**, 579 (2008), arXiv:0710.1002 [hep-th].
- [90] D. J. Toms, *Nature* **468**, 56 (2010), arXiv:1010.0793 [hep-th].
- [91] D. J. Toms, *Phys. Rev.* **D84**, 084016 (2011).
- [92] H. Gies and R. Sondenheimer, *Eur. Phys. J.* **C75**, 68 (2015), arXiv:1407.8124 [hep-ph].
- [93] A. Eichhorn, *Phys. Rev.* **D87**, 124016 (2013), arXiv:1301.0632 [hep-th].
- [94] A. Eichhorn, D. Mesterházy, and M. M. Scherer, *Phys. Rev.* **E88**, 042141 (2013), arXiv:1306.2952 [cond-mat.stat-mech].
- [95] A. Eichhorn, T. Helfer, D. Mesterházy, and M. M. Scherer, *Eur. Phys. J.* **C76**, 88 (2016), arXiv:1510.04807 [cond-mat.stat-mech].
- [96] J. K. Esbensen, T. A. Rytlov, and F. Sannino, *Phys. Rev.* **D93**, 045009 (2016), arXiv:1512.04402 [hep-th].
- [97] A. Beniwal, F. Rajec, C. Savage, P. Scott, C. Weniger, M. White, and A. G. Williams, (2015), arXiv:1512.06458 [hep-ph].
- [98] M. Mitter, J. M. Pawłowski, and N. Strodthoff, *Phys. Rev.* **D91**, 054035 (2015), arXiv:1411.7978 [hep-ph].
- [99] A. K. Cyrol, M. Mitter, J. M. Pawłowski, and N. Strodthoff, in preparation.
- [100] T. Denz, A. Held, J. M. Pawłowski, and A. Rodigast, in preparation.
- [101] M. Reuter and C. Wetterich, *Nucl. Phys.* **B417**, 181 (1994).
- [102] D. F. Litim and J. M. Pawłowski, *JHEP* **0209**, 049 (2002), arXiv:hep-th/0203005 [hep-th].
- [103] D. F. Litim and J. M. Pawłowski, *Phys.Lett.* **B546**, 279 (2002), arXiv:hep-th/0208216 [hep-th].
- [104] I. H. Bridle, J. A. Dietz, and T. R. Morris, *JHEP* **03**, 093 (2014), arXiv:1312.2846 [hep-th].
- [105] D. F. Litim, *Phys.Lett.* **B486**, 92 (2000), arXiv:hep-th/0005245 [hep-th].
- [106] D. F. Litim, *Phys.Rev.* **D64**, 105007 (2001), arXiv:hep-th/0103195 [hep-th].
- [107] H. Gies and S. Lippoldt, *Phys.Rev.* **D89**, 064040 (2014), arXiv:1310.2509 [hep-th].
- [108] S. Lippoldt, *Phys. Rev.* **D91**, 104006 (2015), arXiv:1502.05607 [hep-th].
- [109] P. van Nieuwenhuizen, *Phys. Rev.* **D24**, 3315 (1981).
- [110] R. P. Woodard, *Phys. Lett.* **B148**, 440 (1984).
- [111] H. Gies and C. Wetterich, *Phys.Rev.* **D69**, 025001 (2004), arXiv:hep-th/0209183 [hep-th].